AJ, IN PRESS
Preprint typeset using LaTeX style emulateapj v. 11/26/03

SPECTRAL ENERGY DISTRIBUTIONS AND AGE ESTIMATES OF 104 M31 GLOBULAR CLUSTERS

SONG WANG,[1,2,3] ZHOU FAN,[1] JUN MA,[1,3] RICHARD DE GRIJS,[4,5] XU ZHOU[1]

AJ, in press

ABSTRACT

We present photometry of 104 M31 globular clusters (GCs) and GC candidates in 15 intermediate-band filters of the Beijing-Arizona-Taiwan-Connecticut (BATC) photometric system. The GCs and GC candidates were selected from the Revised Bologna Catalog (v.3.5). We obtain the cluster ages by comparing the photometric data with up-to-date theoretical synthesis models. The photometric data used are *GALEX* far- and near-ultraviolet and 2MASS near-infrared JHK_s magnitudes, combined with optical photometry. The ages of our sample clusters cover a large range, although most clusters are younger than 10 Gyr. Combined with the ages obtained in our series of previous papers focusing on the M31 GC system, we present the full M31 GC age distribution. The M31 GC system contains populations of young and intermediate-age GCs, as well as the 'usual' complement of well-known old GCs, i.e., GCs of similar age as the majority of the Galactic GCs. In addition, young GCs (and GC candidates) are distributed nearly uniformly in radial distance from the center of M31, while most old GCs (and GC candidates) are more strongly concentrated.

Subject headings: galaxies: individual (M31) – galaxies: star clusters – galaxies: stellar content

1. INTRODUCTION

Globular clusters (GCs) are among the oldest known stellar systems in the Universe. They typically have ages similar to those of their host galaxies, thus making them fossils that may provide important information about the formation and evolution of their parent galaxies. In addition, nearly all types of galaxies contain GCs, from dwarfs to giants and from the earliest to the latest types (Fusi Pecci et al. 2005). However, our most in-depth understanding of GC systems has predominantly come from studies of the Milky Way.

M31, located at a distance of $\sim$ 780 kpc (Stanek & Garnavich 1998; Macri 2001), is the largest galaxy in the Local Group. By virtue of the natural advantage of being located at a reasonable distance, the galaxy offers us an ideal environment for detailed, resolved investigations of a large GC system, using both *Hubble Space Telescope (HST)* (e.g., Grillmair et al. 1996; Holland et al. 1997; Rich et al. 2005; Perina et al. 2009b) and ground-based observations with large telescopes (e.g., Christian & Heasley 1991).

A large number of studies focusing on the M31 GC system have been performed since Hubble (1932)'s original identification of 140 GC candidates in M31. The latest Revised Bologna Catalogue of M31 GCs and candidates (hereafter RBC v.3.5) (Galleti et al. 2004, 2006, 2007) was updated on March 27, 2008, and contains 1983 objects (509 confirmed and 1049 candidate GCs, 9 controversial objects, 147 galaxies, 6 HII regions, 245 stars, 5 asterisms, and 13 extended clusters). These objects were observed and discovered by a large number of authors using a variety of observational systems (see, e.g., Vetešnik 1962; Sargent et al. 1977; Battistini et al. 1980; Crampton et al. 1985; Barmby et al. 2000). To obtain a homogeneous photometric data set, Galleti et al. (2004) took the observed data of Barmby et al. (2000) as reference and transformed other observations to this standard setup.

An accurate and reliable analysis of star clusters is important for our understanding of the formation, buildup, and evolutionary processes in galaxies. By comparing integrated photometry with models of simple stellar populations (SSPs), recent studies have achieved some success in determining ages and masses of extragalactic star clusters (e.g., de Grijs et al. 2003a,b,c; de Grijs & Anders 2006; Bik et al. 2003; Ma et al. 2006a; Fan et al. 2006; Ma et al. 2007a, 2009a). Ma et al. (2006a) and Fan et al. (2006) derived age estimates for M31 GCs by fitting SSP models (Bruzual & Charlot 2003, henceforth BC03) to their photometric measurements in a large number of intermediate- and broad-band filters spanning the spectral range from the optical to the near-infrared (NIR). In particular, Ma et al. (2007a) determined an age for the M31 GC S312 (B379), using multicolor photometry from the near-ultraviolet (near-UV) to the NIR, of $9.5^{+1.2}_{-1.0}$ Gyr. S312 (B379) is, in fact, among the first extragalactic GCs for which the age was estimated accurately and independently, using main-sequence photometry, at $10^{+2.5}_{-1}$ Gyr (Brown et al. 2004). This provides a robust check on our methodology to derive age constraints based on the spectral energy distributions (SEDs) of (simple) stellar systems.

This paper is organized as follows. In §2 we present Beijing-Arizona-Taiwan-Connecticut (BATC) observations of our sample GCs and GC candidates, the relevant data-processing steps, and the *GALEX* (far- and near-UV), optical broad-band, and Two-Micron All Sky Survey (2MASS) NIR data that are subsequently used in our analysis. In §3 we derive the ages of our sample clusters by comparing their SEDs with the GALEV SSP models. We then discuss and summarize our results in §4.

2. GC SAMPLE AND BATC INTERMEDIATE-BAND PHOTOMETRY

2.1. *GC sample selection*

To obtain photometry in 15 intermediate-band filters of the BATC photometric system for 61 GCs and GC candidates in the RBC v.3.5, for which few measurements are presently

[1] National Astronomical Observatories, Chinese Academy of Sciences, Beijing, 100012, P. R. China;
majun@bac.pku.edu.cn
[2] Graduate University, Chinese Academy of Sciences, Beijing, 100039, P. R. China
[3] Key Laboratory of Optical Astronomy, National Astronomical Observatories, Chinese Academy of Sciences, Beijing, 100012, China
[4] Kavli Institute for Astronomy and Astrophysics, Peking University, Beijing, 100871, P. R. China
[5] Department of Physics & Astronomy, University of Sheffield, Sheffield S3 7RH, UK

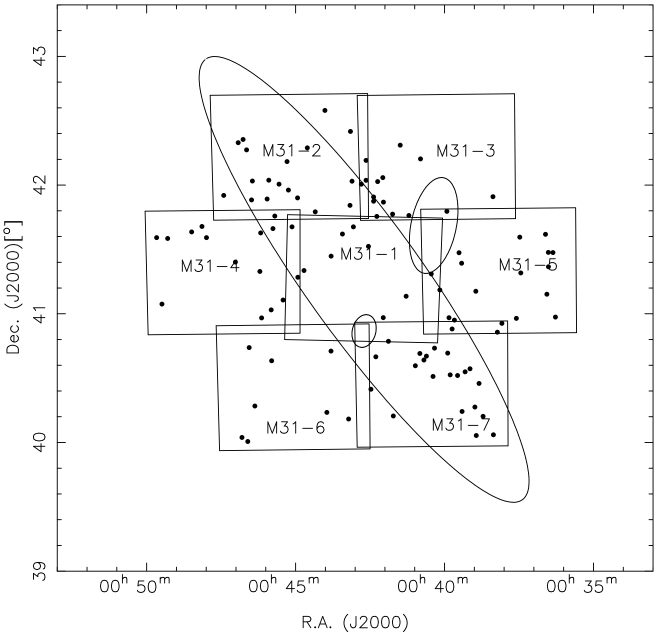

FIG. 1.— BATC observations of our M31 fields. Each field is $58' \times 58'$ (size of the old CCD). The large ellipse is the boundary between the M31 disk and halo (Racine 1991), while the two small ellipses represent the D_{25} isophotes of NGC 205 (northwest) and M32 (southeast). Solid circles indicate the sample GCs and GC candidates discussed in this paper.

available in any photometric system, Fan et al. (2009) mined the BATC survey archive for observations obtained between February 1995 and March 2008. The resulting set of observations covers approximately six square degrees. For the purpose of estimating accurate cluster ages, we selected clusters for which the metallicities and reddening values had been estimated accurately, independently, and homogeneously in previous studies (Huchra et al. 1991; Barmby et al. 2000; Perrett et al. 2002; Fan et al. 2008): see §2.6. We selected classes 1, 2, 3, and 8 (1580 objects) from column 'f' in the RBC v.3.5, which include GCs, candidate GCs, controversial objects, and extended clusters. This resulted in an initial selection of 366 objects. Jiang et al. (2003), Ma et al. (2006a), and Ma et al. (2009a) obtained multicolor photometry for 180 of these GCs and GC candidates. In this paper, we consider the remaining 186 objects. Caldwell et al. (2009) published an updated catalog of 1300 objects in M31, including 670 likely star clusters, with the remaining objects being stars or background galaxies once thought to be clusters (see Tables 3 and 5 of Caldwell et al. 2009). From a comparison with Caldwell et al. (2009), we find that 66 objects are either stars or background galaxies. Therefore, the final sample of M31 GCs and GC candidates analyzed in this paper includes 120 objects. However, we cannot obtain accurate photometric measurements for 16 of these objects because of either a nearby very bright object (B065 and B344D), very faint fluxes superimposed onto a bright background (B119, B396, NB16, and V031), or a location very close to (or blend with) another object (B150D, B176, B256D, B302, B345, B366, B381, B391, and B397), leading to compromised photometric measurements. Object B330 is both faint and located very close to a brighter object. Thus, here we analyze the multicolor photometric properties of 104 GCs and GC candidates. Figure 1 shows their spatial distribution across the M31 fields observed with the BATC multicolor system.

2.2. *BATC intermediate-band photometry*

The observations of our sample GCs and GC candidates were carried out in the BATC photometric system, using the 60/90 cm $f/3$ Schmidt telescope at Xinglong Station of the National Astronomical Observatories of the Chinese Academy Sciences (NAOC). The BATC system includes 15 intermediate-band filters, covering a wavelength range from 3300 Å to 1 μm. The parameters of the filters are given in Table 1, where column (1) gives the filter name, column (2) is the central wavelength for each filter, and column (3) lists the bandwidth for each filter. The 2k×2k CCD used before February 2006 had a pixel size of 15 μm and a resolution of $1.7''$ pixel^{-1}. After February 2006, a new 4k×4k CCD with a pixel size of 12 μm was used, with a resolution of $1.3''$ pixel^{-1} (Fan et al. 2009). The new CCD camera is much more sensitive at short wavelengths.

We obtained 143.9 hours of imaging (447 images) of the M31 field, covering about six square degrees, through the set of 15 filters in five observing runs from 1995 to 2008, spanning 13 years (see for details Fan et al. 2009). The data were reduced using standard procedures, including bias subtraction and flat fielding of the CCD images, with an automatic data-reduction software package (PIPELINE I) specifically developed for the BATC sky survey. BATC magnitudes are defined and obtained in a similar way as for the spectrophotometric AB magnitude system (see for details Ma et al. 2009a). For the *a* to *p* filters of the central field of M31 (M31-1 in Figure 1), the absolute flux of the combined images was obtained using calibrated standard stars, while for the M31-2 to M31-7 fields we used the M31-1 field to derive secondary transformations (see for details Fan et al. 2009).

We determined the magnitudes of our sample objects on the combined images using standard aperture photometry, i.e., using the PHOT routine in DAOPHOT (Stetson 1987). To avoid contamination from nearby objects, we adopted apertures with radii of 3 and 4 pixels on the 2k×2k and 4k×4k CCDs, respectively. For the old CCD, we took 8 and 13 pixels from the object's center as the inner and outer radii of the sky annulus for background determination, while for the new CCD, the corresponding radii were set at 10 and 17 pixels, respectively (Fan et al. 2009). We used isolated stars to obtain point-source aperture corrections by measuring the magnitude differences between the fluxes contained within radii of 3 (4) pixels on the old (new) CCD images and the total stellar magnitudes in each of the 15 BATC filters. The resulting aperture-corrected SEDs for the sample GCs and GC candidates in M31 are provided in Table 2. Columns (2) to (16) represent the magnitudes in the 15 BATC passbands used for our photometry. The 1σ magnitude uncertainties, from DAOPHOT, are listed for each object on the second line for the corresponding passband. For some GCs and GC candidates, the magnitudes in some filters could not obtained because of low signal-to-noise ratios.

2.3. *GALEX UV, optical broad-band, and 2MASS NIR photometry*

To estimate the ages of the M31 GCs and GC candidates, we should ideally use as many photometric data points covering as wide a wavelength range as possible (cf. de Grijs et al. 2003b; Anders et al. 2004; Ma et al. 2009a). The RBC v.3.5 includes *GALEX* (far- and near-UV) fluxes from Rey et al. (2007), optical broad-band, and 2MASS NIR magnitudes for 1983 objects, which we use as the basis for our anal-

ysis. Although the *UBVRI* magnitudes of the objects published by Barmby et al. (2000) are included in the RBC v.3.5 and as such provide the most homogeneous set of photometric measurements available, the relevant photometric uncertainties are not listed. Therefore, we adopt the original *UBVRI* measurements of Barmby et al. (2000), including their published photometric errors. For the remaining objects we adopt the *UBVRI* measurements from the RBC v.3.5. We assign photometric uncertainties following Galleti et al. (2004), i.e., ±0.05 mag in *BVRI* and ±0.08 mag in *U* (see for details Ma et al. 2009a).

In the RBC v.3.5, the 2MASS JHK_s magnitudes were transformed to the CIT photometric system (Galleti et al. 2004). However, we need the original 2MASS JHK_s data to compare the observed SEDs with the SSP models, so we reversed the transformation using the equations given by Carpenter (2001). We obtained the magnitude errors in the JHK_s bands by comparing our photometric data with fig. 2 of Carpenter et al. (2001), which shows the generic photometric uncertainties as a function of magnitude for stars brighter than their observational completeness limits (see for details Ma et al. 2009a). We include the *GALEX*, optical broad-band, and 2MASS NIR photometry of the sample clusters in Table 3 (columns 3 to 12), where the photometric errors are listed for each object on the second line for the corresponding passband. The *GALEX* photometric system is calibrated to match the spectrophotometric AB system, while the optical broad-band and 2MASS photometric data are given in Vega magnitudes. Finally, column 2 includes the classification flags from the RBC v.3.5.

2.4. *Comparison with previously published photometry*

To check our photometry, we transformed the BATC intermediate-band system to the *UBVRI* broad-band system using the relationships between these two systems derived by Zhou et al. (2003):

$$B = m_d + 0.2201(m_c - m_e) + 0.1278 \pm 0.076 \quad \text{and} \qquad (1)$$

$$V = m_g + 0.3292(m_f - m_h) + 0.0476 \pm 0.027. \qquad (2)$$

B-band photometry can be derived from the BATC c, d, and e bands, while *V*-band magnitudes can be obtained from the BATC f, g, and h bands. Figure 2 shows a comparison of the *B* and *V* photometry of our M31 sample objects with previous measurements from Barmby et al. (2000) and Galleti et al. (2004). The mean *B* and *V* magnitude differences—in the sense of this paper minus Barmby et al. (2000) or Galleti et al. (2004)—are $\langle \Delta B \rangle = -0.077 \pm 0.022$ mag and $\langle \Delta V \rangle = -0.047 \pm 0.033$. Our magnitudes are in good agreement with previous *V*-band determinations. However, a significant disagreement becomes apparent in the *B* band for objects with $B > 17.5$ mag. This disagreement has its origin in the difference between our photometry and that of Galleti et al. (2004). In fact, our *B*-band photometry agrees well with that of Barmby et al. (2000), even for $B > 17.5$ mag objects (except for one sample cluster). Referring to Jiang et al. (2003) and Ma et al. (2009a), we also see that our photometric values are fully consistent with Barmby et al. (2000). In Ma et al. (2009a), the analysis of the majority of the GCs was based on the photometric data of Barmby et al. (2000), so even in the *B* band the agreement is good: see fig. 3 of Ma et al. (2009a). We excluded B257 from the comparison,

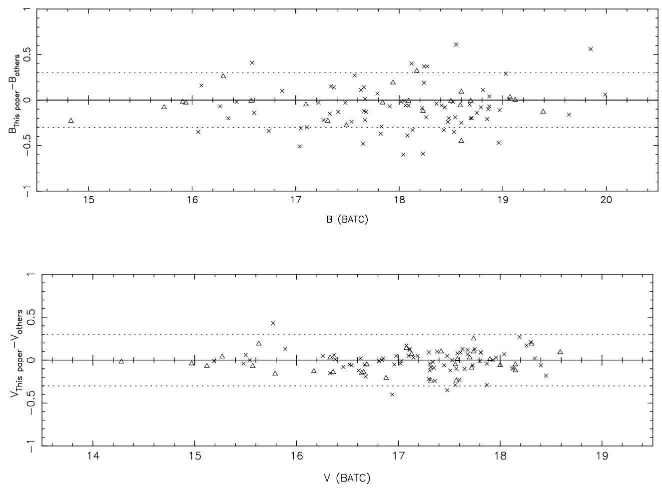

FIG. 2.— Comparison of the photometry of our GCs and GC candidates with previous measurements from Barmby et al. (2000) (triangles) and Galleti et al. (2004) (crosses). The dashed lines enclose ΔV and $\Delta B = 0.3$ mag.

because its *V*-band magnitude is too faint compared with the magnitudes obtained in the other bands (see Table 3). In fact, from the observed SEDs, this photometric measurement is unusually far away from the best-fitting integrated SEDs (see §3 for more details). This data point was taken from Table 4 of Barmby & Huchra (2001), and the offset may be a typical error. Based on the BATC f, g, and h magnitudes, we obtain $V = 17.76$ mag for B257. Note that the *B*-band magnitude of this cluster as listed in Table 4 of Barmby & Huchra (2001) is 11.907, which is too bright for any reasonable SED and may also be a typical uncertainty.

2.5. *Metallicities and reddening values*

We require independently (but homogeneously) determined metallicities and reddening values to robustly and accurately estimate the ages of our sample objects. We used three homogeneous sources of spectroscopic metallicities (Huchra et al. 1991; Barmby et al. 2000; Perrett et al. 2002) and one homogenized reference (see for details Fan et al. 2008; Ma et al. 2009a).

Following Ma et al. (2009a), for reasons of consistency we ranked the sources used to assign metallicities to our M31 GCs in order of preference. Metallicities from Perrett et al. (2002) were chosen whenever available because of the large number of their metallicity determinations, followed (in order) by metallicity determinations from Barmby et al. (2000) and Huchra et al. (1991). If none of these three sources included spectroscopic metallicities for a given sample cluster, we used the corresponding value from Fan et al. (2008).

For reddening values, we used Barmby et al. (2000) and Fan et al. (2008) as our reference (see for details Ma et al. 2009a). Because the reddening values from Fan et al. (2008) comprise a homogeneous data set and the number of GCs included is greater than that of Barmby et al. (2000), we preferentially adopt Fan et al. (2008) reddening values, followed by those of Barmby et al. (2000), in a similar approach as adopted by Ma et al. (2009a). The metallicities and reddening values adopted for our sample clusters are listed in Table 4.

3. AGE DETERMINATION

An SSP is defined as a single generation of coeval stars characterized by the same parameters, including metallicity,

age, and stellar initial mass function (IMF). SSP models are calculated on the basis of a set of evolutionary tracks of stars of different initial masses, combined with stellar spectra at different evolutionary stages. In this paper, and following Ma et al. (2009a), we compare the SEDs of our sample objects with the GALEV SSP models (e.g., Kurth et al. 1999; Schulz et al. 2002; Anders & Fritze-v. Alvensleben 2003) to estimate their ages. The GALEV SSPs are based on the Padova isochrones (covering wavelengths from 91 Å to 160 μm) and a Salpeter (1955) stellar IMF with lower and upper mass limits of 0.10 $M_\odot$ and 50–70 $M_\odot$, respectively (the latter depending on metallicity). These models cover ages from 4 Myr to 16 Gyr, with an age resolution of 4 Myr for ages younger than 2.35 Gyr, and 20 Myr for older ages. We convolved the theoretical SSP SEDs with the *GALEX*, broad-band $UBVRI$, BATC intermediate-band, and 2MASS JHK_s filter response curves to obtain synthetic UV, optical, and NIR photometry (Ma et al. 2009a). The synthetic magnitude in the AB magnitude system for the $i^{\rm th}$ filter is

$$m_i = -2.5 \log \frac{\int_\nu F_\nu \varphi_i(\nu) {\rm d}\nu}{\int_\nu \varphi_i(\nu) {\rm d}\nu} - 48.60, \quad (3)$$

where F_ν is the theoretical SSP SED (which is a function of age and metallicity) and φ_i is the response curve of the $i^{\rm th}$ filter. The GALEV SSP models include five initial metallicities, $Z = 0.0004, 0.004, 0.008, 0.02$ (solar), and 0.05. For other metallicities, the relevant spectra can be obtained by linear interpolation of the appropriate model spectra for any of these five metallicities. For metallicities below $Z = 0.0004$ we use the $Z = 0.0004$ model (Ma et al. 2009a).

To determine the most compatible GALEV SSP model for a given observed SED, we adopted a χ^2 minimization test,

$$\chi^2 = \sum_{i=1}^{25} \frac{[m_{\nu_i}^{\rm intr} - m_{\nu_i}^{\rm mod}(t)]^2}{\sigma_i^2}, \quad (4)$$

where $m_{\nu_i}^{\rm mod}(t)$ is the magnitude in the $i^{\rm th}$ filter of a theoretical SSP at age t, while $m_{\nu_i}^{\rm intr}$ is the intrinsic (observed and corrected) magnitude in the same filter. The interstellar extinction curve A_ν is taken from Cardelli et al. (1989), $R_\nu = A_V/E_{B-V} = 3.1$. σ_i is the magnitude uncertainty in the $i^{\rm th}$ filter, defined as

$$\sigma_i^2 = \sigma_{{\rm obs},i}^2 + \sigma_{{\rm mod},i}^2. \quad (5)$$

Here, $\sigma_{{\rm obs},i}$ and $\sigma_{{\rm mod},i}$ are the observational uncertainty and that associated with the model itself, respectively. Charlot et al. (1996) estimated $\sigma_{{\rm mod},i}$ by comparing the colors obtained from different stellar evolutionary tracks and spectral libraries. We adopt $\sigma_{{\rm mod},i} = 0.05$ mag, following Wu et al. (2005), Ma et al. (2006a, 2009a), and Fan et al. (2006). The SED fits of our sample GCs and GC candidates are shown in Fig. 3.

4. RESULTS AND SUMMARY

In §3 we determined the ages of 104 GCs and GC candidates in M31. The results are tabulated in Table 5. Figure 4 shows the age distribution of the sample clusters, from which we conclude that, except for 20 clusters, the ages of most sample GCs are between 1 and 5 Gyr, with a peak at $\sim$ 2 Gyr. The 'usual' complement of well-known old GCs (i.e., GCs of similar age as the majority of the Galactic GCs) is also present. In addition, while fitting SSP models to the observed data, we found that some photometric data of a small number of clusters cannot be fitted with any SSP models. We therefore did not use these deviating photometric data points to obtain the best fits. This applies to the *GALEX* far-UV data of B138D, the 2MASS K_s, H, and J magnitudes of B142D, B181D, and B289D, respectively, the B-band and 2MASS H fluxes of B245D, and the V-band magnitude of B257.

Other authors have also considered the age distribution of the GCs in M31. For example, Barmby et al. (2000) discovered that M31 contains GCs exhibiting strong Balmer lines and A-type spectra, from which one infers that these objects must be very young. Beasley et al. (2004) and Puzia et al. (2005) confirmed this conclusion. Burstein et al. (2004) and Fusi Pecci et al. (2005) carefully studied the sample of young M31 GCs. Very recently, Caldwell et al. (2009) determined the ages and reddening values of 140 young clusters in M31 by comparing the observed spectra with models, and found that these clusters are less than 2 Gyr old, while most clusters have ages between 10^8 and 10^9 yr. Perina et al. (2009a) estimated an age for VDB0-B195D of $\sim$ 25 Myr based on *HST*/WFPC2 color-magnitude diagrams (CMDs). The ages of the M31 clusters determined in this paper are in general agreement with previous determinations, which we will show in more detail below on the basis of comparisons between our determinations and previous age estimates for individual objects.

The most direct and most accurate method to determine a cluster's age is by means of main-sequence photometry, since the absolute magnitude of the main-sequence turnoff is a strong function of age. Williams & Hodge (2001a,b) estimated ages of many young disk clusters in M31 based on *HST*/WFPC2 CMDs and isochrone fitting to either the main sequence or luminous evolved stars. Only one of their clusters (B315) is in common with our sample. They obtained an age of $\sim$ 0.1 Gyr for this cluster, while we determined it to be approximately 0.5 Gyr old. Both age determinations are mutually consistent within the uncertainties. Caldwell et al. (2009) compared their ages with those of Williams & Hodge (2001a,b) and concluded that both sets of age determinations were in good agreement. We therefore compare our ages with Caldwell et al. (2009) for the seven clusters we have in common with their sample (B018, B307, B316, B448, B475, B483, and V031: see Table 6). It is evident that they are largely internally consistent. Puzia et al. (2005) also presented spectroscopic ages, metallicities, and [α/Fe] ratios for 70 M31 GCs based on Lick line-index measurements. A cross correlation with Puzia et al. (2005)'s sample shows that we have 21 clusters in common. A direct comparison shows that the ages of Puzia et al. (2005) are systematically older than ours. This surprising result prompted us to compare the ages of clusters in common between Puzia et al. (2005) and other authors (Williams & Hodge 2001a,b; Beasley et al. 2004; Caldwell et al. 2009). We found similar systematic offsets (see for details also Ma et al. 2009a).

We have determined the ages of M31 GCs and GC candidates in a series of previous papers (Jiang et al. 2003; Ma et al. 2006a,b; Fan et al. 2006; Ma et al. 2007a, 2009a,b) based on the same method as used in the present paper, i.e., by constructing SEDs of known M31 GC candidates and using the SED shapes to estimate cluster ages. In the first paper of this series, Jiang et al. (2003) estimated the ages of 172 M31 GC candidates based on photometric measurements in 13 BATC intermediate-band filters and the SSP models of Bruzual & Charlot (1996; unpublished, hereafter BC96). Subsequently,

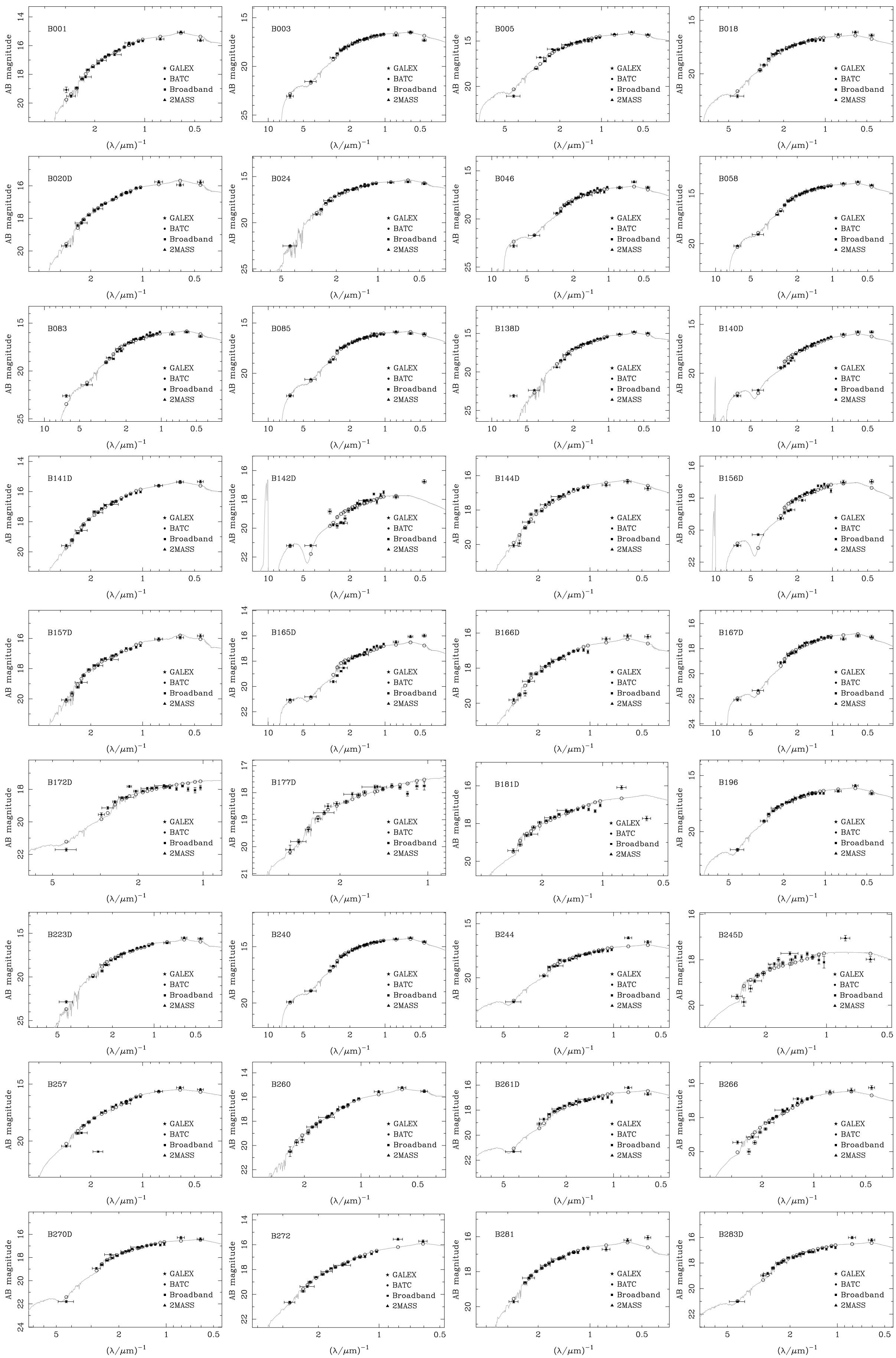

FIG. 3.— SED fits of the GALEV SSP models to our sample objects.

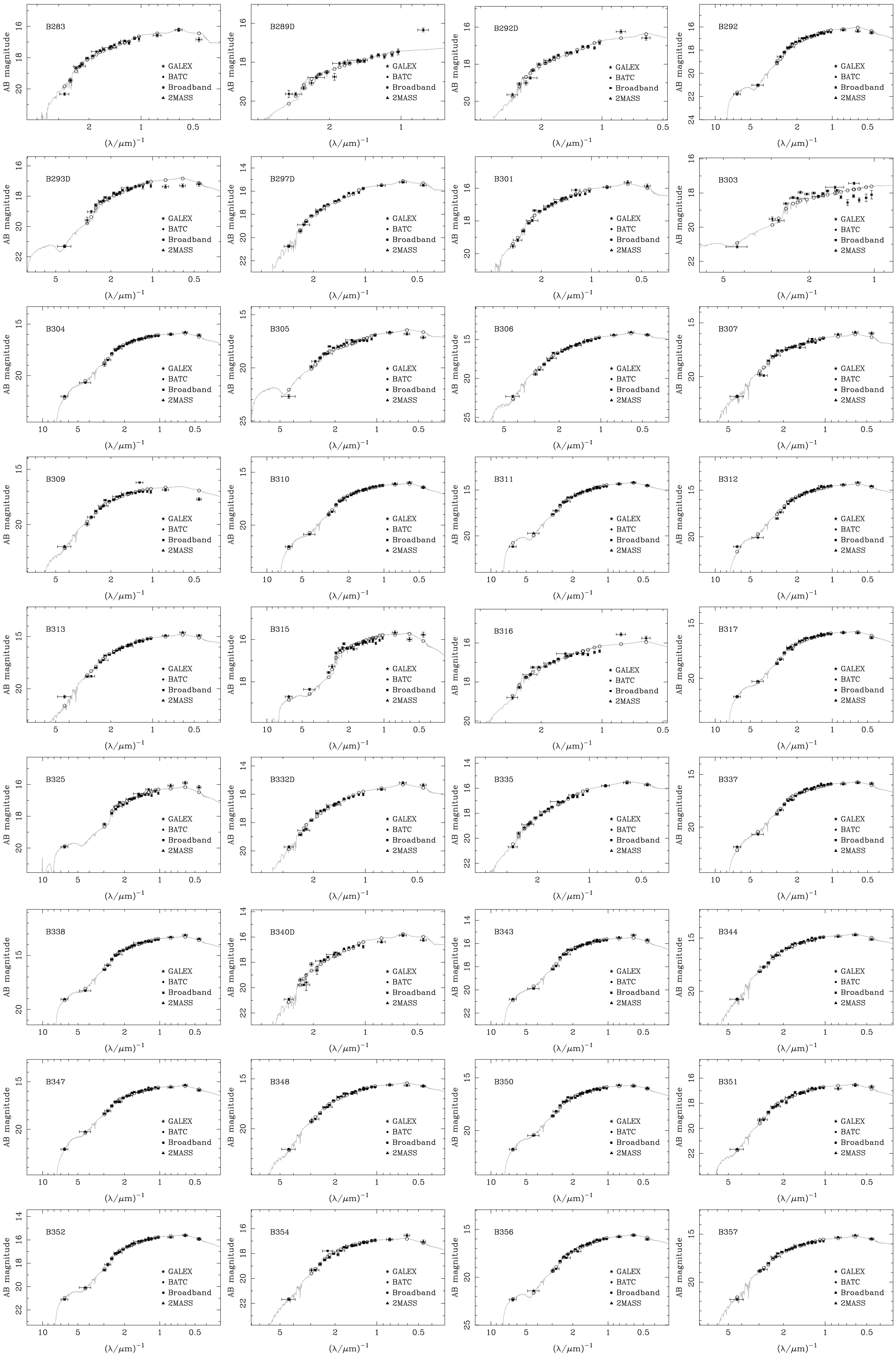

FIG. 3.— Continued.

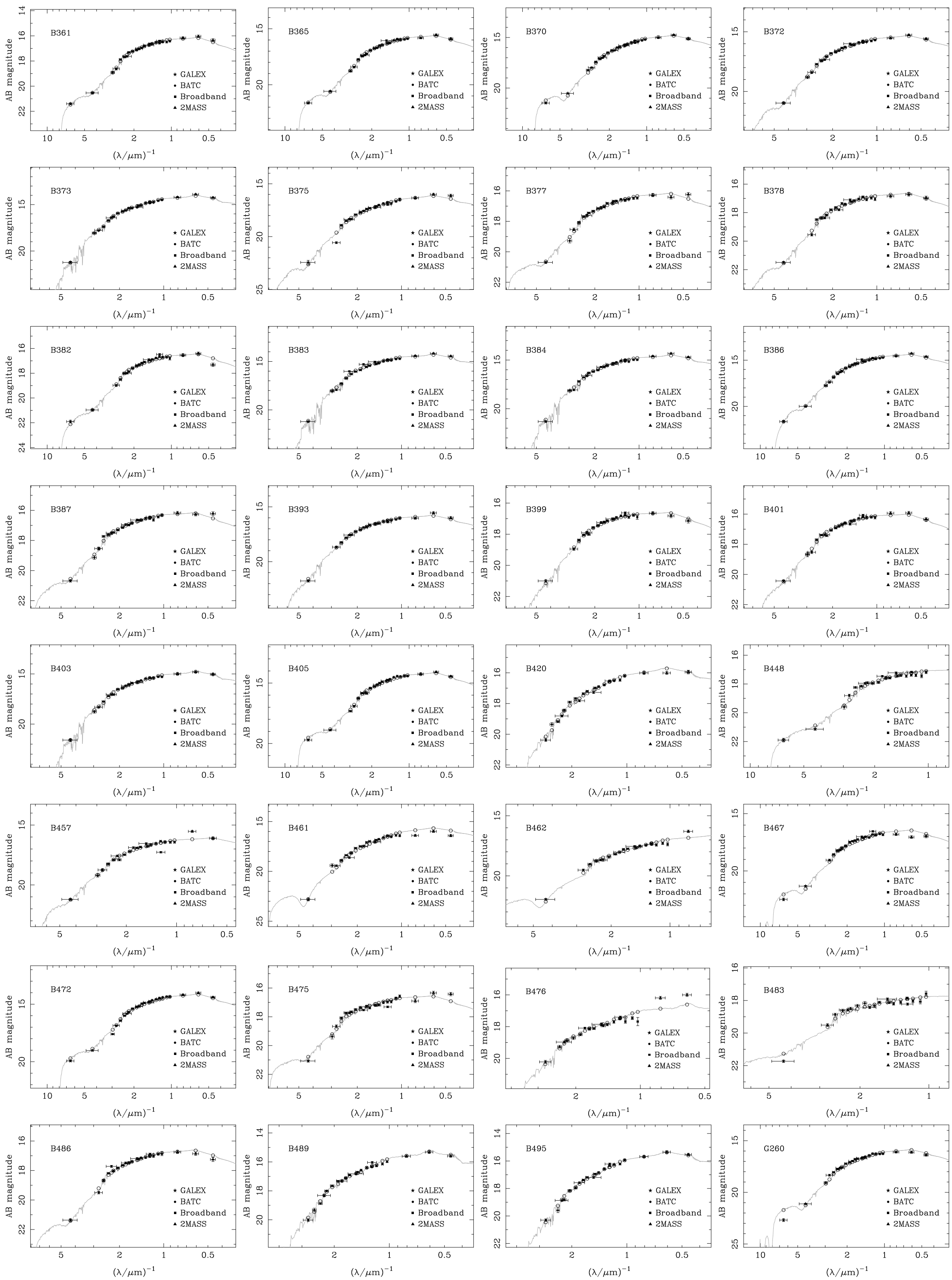

FIG. 3.— Continued.

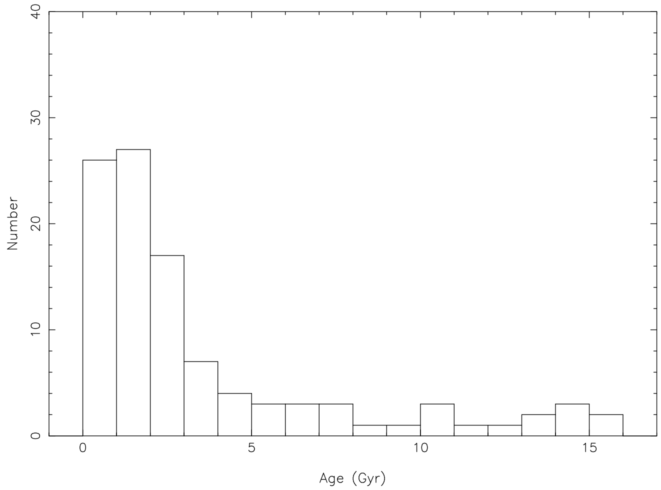

FIG. 4.— Age distribution of our sample GCs and GC candidates in M31.

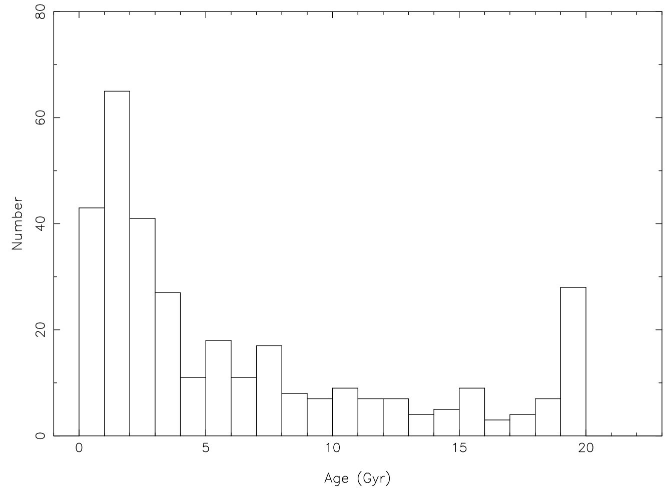

FIG. 5.— Homogenized age distribution of the 331 M31 GCs and GC candidates discussed in our series of papers.

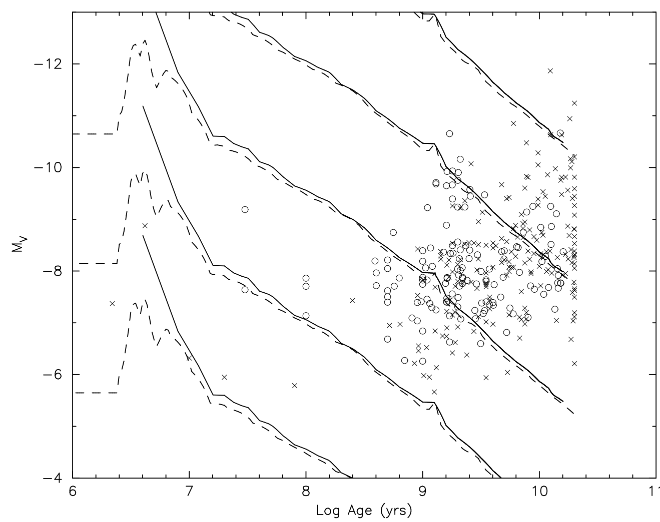

FIG. 6.— Absolute V-band magnitudes for the M31 GCs and GC candidates as a function of age. Overplotted are theoretical lines corresponding to (from bottom to top) masses of 10^2, 10^3, 10^4, 10^5 and $10^6 M_\odot$ from BC03 (dashed line) and GALEV (solid line), respectively.

Fan et al. (2006) obtained new age estimates for 91 GCs from the Jiang et al. (2003) sample, based on improved photometric data including intermediate- and broad-band magnitudes from the optical to the NIR, and the SSP models of BC03. Ma et al. (2006b) then estimated the ages of 33 M31 GC candidates using photometry in 13 BATC intermediate-band filters and the BC03 SSP models, while Ma et al. (2009a) determined the ages of 35 M31 GCs and GC candidates based on photometry including far- and near-UV *GALEX* observations, *UBVRI*, 13 BATC intermediate-band filters, and 2MASS JHK_s, combined with the GALEV SSP models. Ma et al. (2006a, 2007a, 2009b) determined the ages of three specific M31 GCs (037-B327, S312, and G1) based on the BC03 SSP models and a large number of photometric measurements. We determined the ages of these three M31 GCs for special reasons: S312 is among the first extragalactic GCs whose age was estimated accurately using main-sequence photometry, while 037-B327 and G1 are among the most massive GCs in the Local Group. They have been speculated to be nucleated dwarf galaxies instead of genuine GCs (see for detailed discusions Ma et al. 2006c, 2007b). In this series of seven articles, we published ages for 331 different M31 GCs and GC candidates. Figure 5 show the age distribution of these 331 objects. We see that $\sim$ 40 clusters are younger than 1 Gyr. The ages range from $<$ 1 to 20 Gyr (the upper age limit in the BC96 and BC03 SSP models). A population of young clusters, peaking at $\sim$ 3 Gyr, is also apparent.

Figure 6 shows the absolute magnitudes of our sample of M31 GCs and GC candidates as a function of their age. The crosses indicate that the ages are from Jiang et al. (2003), Ma et al. (2006a,b, 2007a, 2009a), and Fan et al. (2006), which were obtained based on the SSP models of BC96 or BC03, while the circles mean that the ages are from Ma et al. (2009a) and the present paper, obtained on the basis of the GALEV SSP models. The dashed and solid lines represent SSP models with $Z = 0.004$ taken from BC03 and GALEV, respectively, for masses of 10^2, 10^3, 10^4, 10^5, and $10^6 M_\odot$ and assuming a Salpeter stellar IMF. The V-band photometry is from the RBC v.3.5. The absolute magnitudes have been corrected for extinction (Barmby et al. 2000; Fan et al. 2008), except for 037-B327, S312, and G1, the reddening values of which are from Ma et al. (2006a), Ma et al. (2007a), and Ma et al. (2009b), respectively. We adopt a distance modulus of $(m - M)_0 = 24.47$ mag (McConnachie et al. 2005). Figure 6 shows that the majority of the clusters have masses between 10^3 and $10^6 M_\odot$.

The distribution of absolute V magnitude of GCs in M31 is shown in Figure 7. Overall, the distribution has a cutoff at the faint end with a magnitude limit of about −5.5 mag (with a few fainter clusters still visible, probably because of advantageous positions, e.g., observable through a hole in the extinction distribution). The various cluster ages are separated in Figure 8, which are: (i) very young ($t < 1$ Gyr), (ii) young ($1 \leq t < 4$ Gyr), (iii) intermediate-age ($4 \leq t < 10$ Gyr), and (iv) old GCs and GC candidates ($t \geq 10$ Gyr). We do not see a clear trend between age and brightness. However, the youngest clusters are not the most massive objects, implying that the conditions in the M31 have not been conducive to massive cluster formation in the recent past.

We converted the absolute magnitudes of our M31 GC sample to photometric masses using the appropriate age-dependent mass-to-light ratios provided by the BC03 and GALEV SSP models. The GC mass versus age diagram is shown in Figure 9. The crosses indicate that the ages are from Jiang

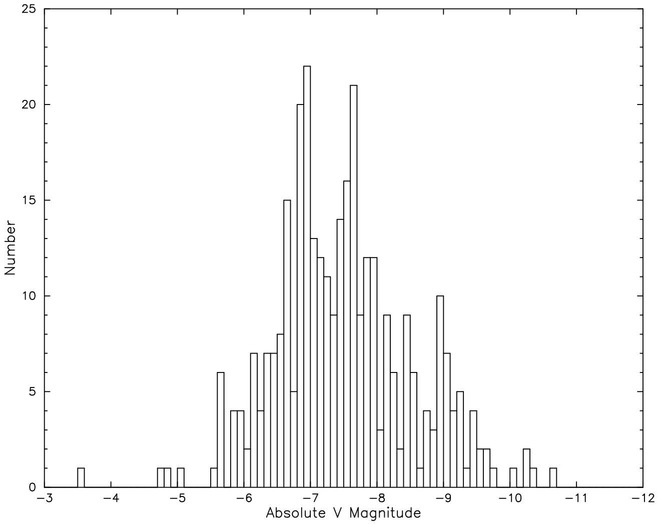

FIG. 7.— Histogram of the absolute V magnitude for the 331 sample GCs and GC candidates in M31.

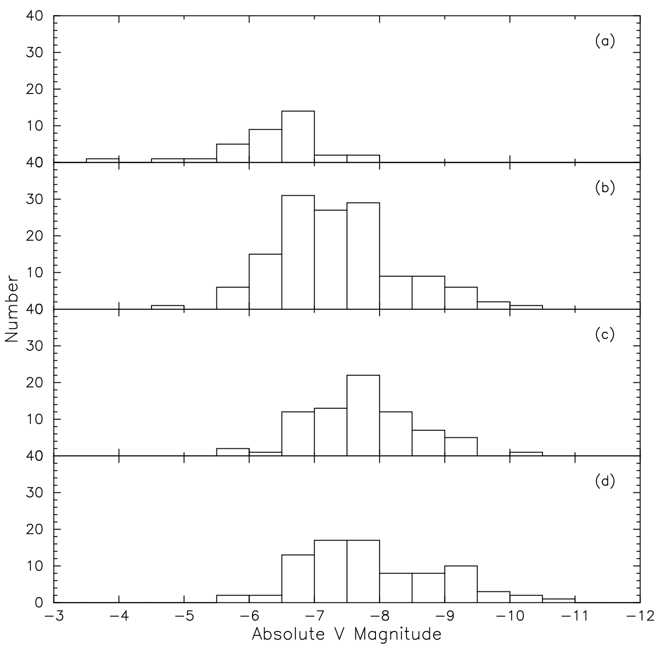

FIG. 8.— Histogram of the absolute V magnitude for the M31 GCs and GC candidates: (a) very young ($t < 1$ Gyr), (b) young ($1 \le t < 4$ Gyr), (c) intermediate-age ($4 \le t < 10$ Gyr), and (d) old GCs and GC candidates ($t \ge 10$ Gyr).

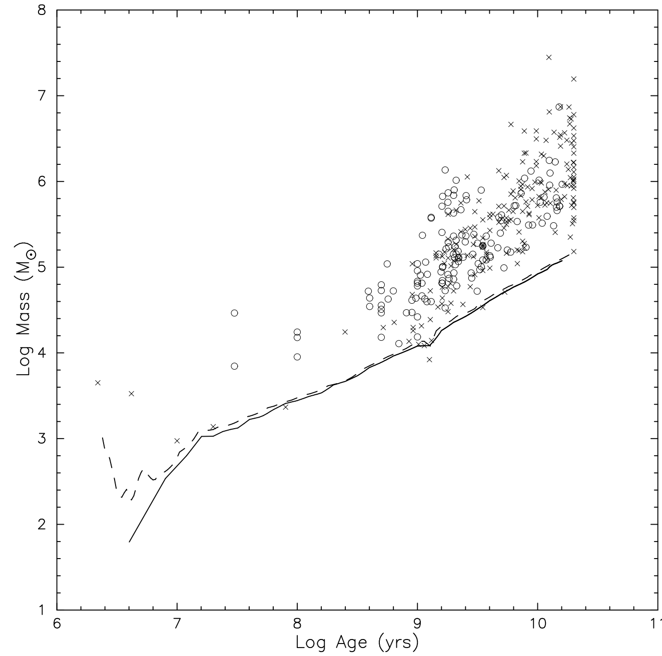

FIG. 9.— Distribution of the M31 GCs and GC candidates in the age-versus-mass plane. Overplotted is the fading limit, based on the observed $M_V = -5.5$ mag sample cutoff and the fading function from the cluster evolutionary models with $Z = 0.004$ taken from BC03 (dashed line) and GALEV (solid line), assuming a Salpeter stellar IMF.

et al. (2003), Ma et al. (2006a,b, 2007a, 2009a), and Fan et al. (2006), and the masses were obtained based on the SSP models of BC03, while the circles mean that the ages are from Ma et al. (2009a) and the present paper, and the masses were obtained on the basis of the GALEV SSP models. Overplotted is the fading limit, assuming $M_{V,\mathrm{limit}} = -5.5$ mag and evolutionary fading based on the $Z = 0.004$ BC03 (dashed line) and GALEV (solid line) models, assuming a Salpeter stellar IMF. Figure 9 shows that our observational ($\sim 50\%$) completeness limit describes the lower mass limit of the entire GC sample up to the oldest ages very well. Similarly, the upper envelope of the points in Figure 9 is likely a result of the 'size-of sample effect' (e.g., Gieles & Bastian 2008, and references therein). It is clear, however, that massive star cluster formation halted abruptly in the disk of M31 approximately 1 Gyr ago. Given that massive ($> 10^4 M_\odot$) young (< 1 Gyr-old) clusters will be significantly brighter than the much older GC-type counterparts in M31, we would have expected any such young massive clusters to have been detected in M31, yet they have not.

Using these 331 GCs and GC candidates with homogeneously determined ages, we can now investigate their spatial distribution. We use an X, Y projection to refer to the relative positions of the objects. Our adopted X coordinate projects along M31's major axis, where positive X increases towards the northeast, while the Y coordinate extends along the minor axis of the M31 disk, increasing towards the northwest. To obtain the relative coordinates of the M31 clusters, we adopted $\alpha_0 = 00^{\rm h}42^{\rm m}44^{\rm s}.30$ and $\delta_0 = +41^\circ16'09''.0$ (J2000.0) for M31's center, following Huchra et al. (1991) and Perrett et al. (2002). Formally,

$$X = A \sin\theta + B\cos\theta \quad \text{and} \tag{6}$$

$$Y = -A\cos\theta + B\sin\theta, \tag{7}$$

where $A = \sin(\alpha - \alpha_0)\cos\delta$ and $B = \sin\delta\cos\delta_0 - \cos(\alpha - \alpha_0)\cos\delta\sin\delta_0$. We adopt a position angle of $\theta = 38^\circ$ for the major axis of M31 (Kent 1989). We divided the GCs and GC candidates into four age groups: (i) very young ($t < 1$ Gyr), (ii) young ($1 \le t < 4$ Gyr), (iii) intermediate-age ($4 \le t < 10$ Gyr), and (iv) old GCs and GC candidates ($t \ge 10$ Gyr). Figure 10 shows their spatial distributions. Although our sample of M31 GCs and GC candidates is not complete (in spatial, radial terms, given that we are limited by the six observed fields), we note that there is a tendency for young GCs and GC candidates to be nearly uniformly distributed around M31. The majority of old GCs appear to occupy the central regions of the galaxy, although this restricted distribution may

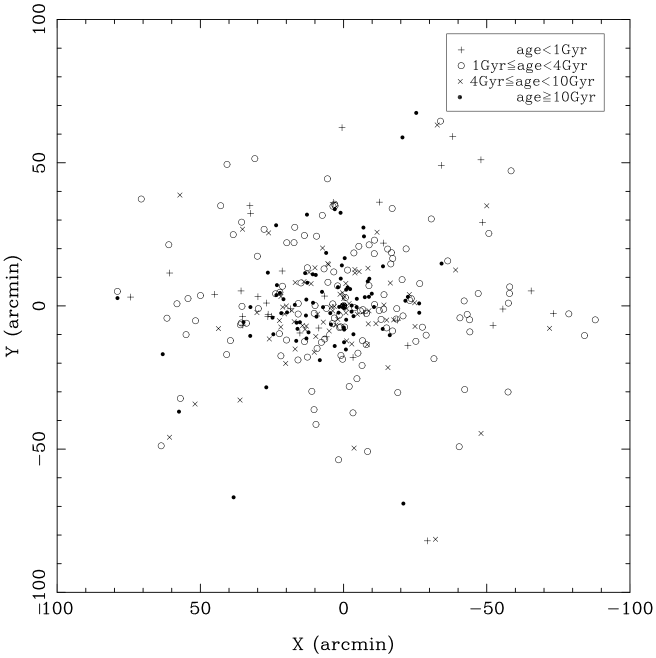

FIG. 10.— Spatial distribution of the M31 GCs and GC candidates: very young ($t < 1$ Gyr), young ($1 \le t < 4$ Gyr), intermediate-age ($4 \le t < 10$ Gyr) and old GCs and GC candidates ($t \ge 10$ Gyr).

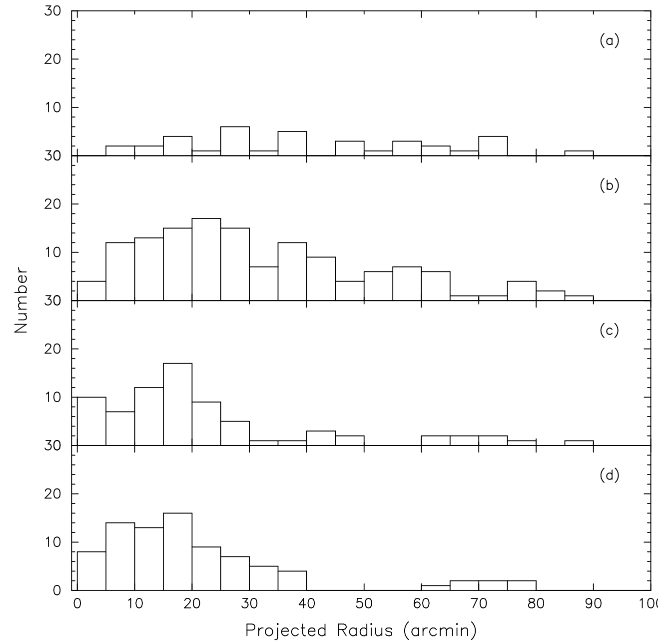

FIG. 11.— Radial distribution of the M31 GCs and GC candidates: (a) very young ($t < 1$ Gyr), (b) young ($1 \le t < 4$ Gyr), (c) intermediate-age ($4 \le t < 10$ Gyr), and (d) old GCs and GC candidates ($t \ge 10$ Gyr).

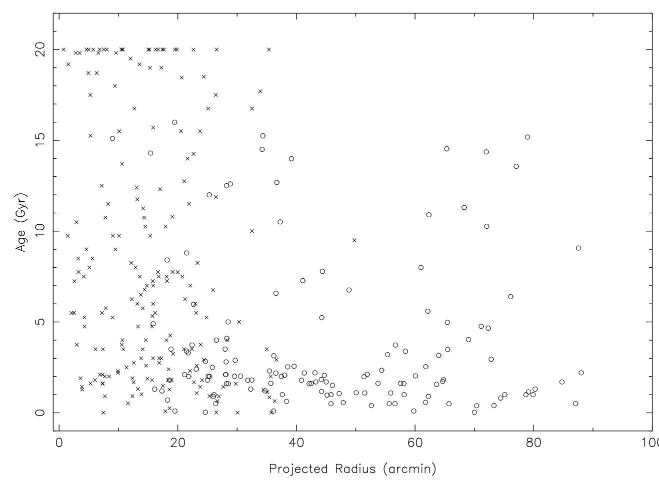

FIG. 12.— Age versus projected galactocentric radius for 331 M31 GCs and GC candidates.

be caused by selection biases. Figure 11 shows the number of GCs and GC candidates as a function of projected radial distance from the M31 center, confirming our conclusions derived from Figure 10. Figure 12 displays the cluster ages as a function of projected radial distance. The crosses indicate that the ages are from Jiang et al. (2003), Ma et al. (2006a,b, 2007a, 2009b), and Fan et al. (2006), which were obtained using the BC96 or BC03 SSP models, while the circles indicate that the ages are from Ma et al. (2009a) and the present paper, obtained on the basis of the GALEV SSP models. Figure 12 shows that young GCs and GC candidates are distributed nearly uniformly, and that most of the old GCs (and candidates) are more concentrated.

This paper presents photometry of 104 M31 globular clusters (GCs) and GC candidates in 15 intermediate-band filters of the BATC photometric system. The age of the clusters were obtained by comparing the photometric data with the theoretical synthesis models. The ages of our sample clusters cover a large range, although most clusters are younger than 10 Gyr. Combined with the ages obtained in our series of previous papers focusing on the M31 GC system, we present the full M31 GC age distribution. The results show that the M31 GC system contains populations of young and intermediate-age GCs, as well as the 'usual' complement of well-known old GCs, i.e., GCs of similar age as the majority of the Galactic GCs. In addition, young GCs (and GC candidates) are distributed nearly uniformly in radial distance from the center of M31, while most old GCs (and GC candidates) are more strongly concentrated.

We are indebted to the referee for thoughtful comments and insightful suggestions that improved this paper significantly. This work was supported by the Chinese National Natural Science Foundation (grants 10873016, 10633020, 10603006, and 10803007) and by National Basic Research Program of China (973 Program; grant 2007CB815403).

REFERENCES

Anders, P., & Fritze-v. Alvensleben, U. 2003, A&A, 401, 1063
Anders, P., Bissantz, N., Fritze-v. Alvensleben, U., & de Grijs, R. 2004, MNRAS, 347, 196
Barmby, P., Huchra, J., Brodie, J., Forbes, D., Schroder, L., & Grillmair, C. 2000, AJ, 119, 727
Barmby, P., & Huchra, J. P. 2001, AJ, 122, 2458
Battistini, P., Bònoli, F., Braccesi, A., Fusi Pecci, F., Malagnini, M. L., & Marano, B. 1980, A&AS, 42, 357
Beasley, M. A., et al. 2004, AJ, 128, 1623
Bik, A., Lamers, H. J. G. L. M., Bastian, N., Panagia, N., & Romaniello, M. 2003, A&A, 397, 473
Brown, T. M., et al. 2004, ApJ, 613, L125

TABLE 1
BATC FILTER PARAMETERS

Filter	Central wavelength (Å)	Bandwidth (Å)
a	3360	360
b	3890	340
c	4210	320
d	4550	340
e	4925	390
f	5270	340
g	5795	310
h	6075	310
i	6660	480
j	7050	300
k	7490	330
m	8020	260
n	8480	180
o	9190	260
p	9745	270

Bruzual, A. G., & Charlot, S. 2003, MNRAS, 344, 1000 (BC03)
Burstein, D., et al. 2004, ApJ, 614, 158
Caldwell, N., Harding, P., Morrison, H., Rose, J. A., Schiavon, R., & Kriessler, J. 2009, AJ, 137, 94
Cardelli, J. A., Clayton, G. C., & Mathis, J. S. 1989, ApJ, 345, 245
Carpenter, J. M. 2001, AJ, 121, 2851
Carpenter, J. M., Hillenbrand, L. A., & Skrutskie, M. F. 2001, AJ, 121, 3160
Charlot, S., Worthey, G., & Bressan, A. 1996, ApJ, 457, 625
Christian, C. A., & Heasley, J. N. 1991, AJ, 101, 848
Crampton, D., Cowley, A. P., Schade, D., & Chayer, P. 1985, ApJ, 288, 494
de Grijs, R., Bastian, N., & Lamers, H. J. G. L. M. 2003a, MNRAS, 340, 197
de Grijs, R., Fritze-v. Alvensleben, U., Anders, P., Gallagher, J. S., Bastian, N., Taylor, V. A., & Windhorst, R. A. 2003b, MNRAS, 342, 259
de Grijs, R., Anders, P., Lynds, R., Bastian, N., Lamers, H. J. G. L. M., & O'Neill, E. J. Jr. 2003c, MNRAS, 343, 1285
de Grijs, R., & Anders, P. 2006, MNRAS, 366, 295
Fan, Z., Ma, J., de Grijs, R., Yang, Y., & Zhou, X. 2006, MNRAS, 371, 1648
Fan, Z., Ma, J., de Grijs, R., & Zhou, X. 2008, MNRAS, 385, 1973
Fan, Z., Ma, J., & Zhou, X. 2009, RAA, 9, 993
Fukugita, M., et al. 1996, AJ, 111, 1748
Fusi Pecci, F., Bellazzini, M., Buzzoni, A., De Simone, E., Federici, L., & Galleti, S. 2005, AJ, 130, 554
Galleti, S., Federici, L., Bellazzini, M., Fusi Pecci, F., & Macrina, S. 2004, A&A, 426, 917
Galleti, S., Federici, L., Bellazzini, M., Buzzoni, A., & Fusi Pecci, F. 2006, A&A, 456, 985
Galleti, S., Bellazzini, M., Federici, L., Buzzoni, A., & Fusi Pecci, F. 2007, A&A, 471, 127
Gieles, M., & Bastian, N. 2008, A&A, 482, 165
Grillmair, C. J., Ajhar, E. A., Faber, S. M., Baum, W. A., Holtzman, J. A., Lauer, T. R., Lynds, C. R., & O'Neil, E. J., Jr. 1996, AJ, 111, 2293
Harris, W. E. 1991, ARA&A, 29, 543
Holland, S., Fahlman, G. G., & Richer, H. B. 1997, AJ, 114, 1488
Hubble, E. P. 1932, ApJ, 76, 44
Huchra, J. P., Brodie, J. P., & Kent, S. M. 1991, ApJ, 370, 495
Jiang, L., Ma, J., Zhou, X., Chen, J., Wu, H., & Jiang Z. 2003, AJ, 125, 727
Kent, S. 1989, AJ, 97, 1614
Kurth, O. M., Fritze-v. Alvensleben, U., & Fricke, K. J. 1999, A&AS, 138, 19
Ma, J., de Grijs, R., Yang, Y., Zhou, X., Chen, J., Jiang, Z., Wu, Z., & Wu, J. 2006a, MNRAS, 368, 1443
Ma, J., et al. 2006b, A&A, 449, 143
Ma, J., et al. 2006c, ApJ, 636, L93
Ma, J., et al. 2007a, ApJ, 659, 359
Ma, J., et al. 2007b, MNRAS, 376, 1621
Ma, J., et al. 2009a, AJ, 137, 4884
Ma, J., et al. 2009b, RAA, 9, 641
McConnachie, A. W., Irwin, M. J., Ferguson, A. M. N., Ibata, R. A., Lewis, G. F., & Tanvir, N. 2005, MNRAS, 356, 979
Macri, L. M. 2001, ApJ, 549, 721
Perrett, K. M., Bridges, T. J., Hanes, D. A., Irwin, M. J., Brodie, J. P., Carter, D., Huchra, J. P., & Watson, F. G. 2002, AJ, 123, 2490
Perina, S. et al. 2009a, A&A, 494, 933
Perina, S. et al. 2009b, A&A, in press (arXiv:0910.0204)
Puzia, T. H., Perrett, K. M., & Bridges, T. J. 2005, A&A, 434, 909
Racine, R. 1991, AJ, 101, 865
Rey, S. C., et al. 2007, ApJS, 173, 643
Rich, R. M., Corsi, C. E., Cacciari, C., Federici, L., Fusi Pecci, F., Djorgovski, S. G., & Freedman, W. L. 2005, AJ, 129, 2670
Salpeter, E. E. 1955, ApJ, 121, 161
Sargent, W. L. W., Kowal, C. T., Hartwick, F. D. A., & van den Bergh, S. 1977, AJ, 82, 947
Schulz, J., Fritze-v. Alvensleben, U., Möller, C. S., & Fricke, K. J. 2002, A&A, 392, 1
Stanek K. Z., & Garnavich, P. M. 1998, ApJ, 503, 131
Stetson, P. B. 1987, PASP, 99, 191
Vetešnik, M. 1962, Bull. Astron. Inst. Czech., 13, 180
Williams, B. F., & Hodge, P. W. 2001a, ApJ, 548, 190
Williams, B. F., & Hodge, P. W. 2001b, ApJ, 559, 851
Wu, H., Shao, Z. Y., Mo, H. J., Xia, X. Y., & Deng, Z. G. 2005, ApJ, 622, 244
Zhou, X., et al. 2003, A&A, 397, 361

TABLE 2
BATC INTERMEDIATE-BAND PHOTOMETRY (MAGNITUDES) OF 104 M31 GCS AND GC CANDIDATES.

Object	*a*	*b*	*c*	*d*	*e*	*f*	*g*	*h*	*i*	*j*	*k*	*m*	*n*	*o*	*p*
B001	19.08	18.94	18.32	17.68	17.49	17.23	16.78	16.65	16.37	16.28	16.10	15.89	15.89	15.72	15.67
	0.190	0.045	0.022	0.038	0.032	0.016	0.021	0.011	0.008	0.013	0.012	0.011	0.016	0.021	0.019
B003	...	18.67	18.35	18.01	17.93	17.74	17.38	17.28	17.15	17.10	16.98	16.85	16.80	16.77	16.69
	...	0.039	0.022	0.045	0.046	0.023	0.031	0.019	0.015	0.024	0.024	0.021	0.043	0.044	0.051
B005	18.07	17.23	16.66	16.01	15.94	15.78	15.43	15.32	15.08	15.05	14.90	14.86	14.86	14.68	14.62
	0.037	0.019	0.017	0.016	0.012	0.010	0.010	0.008	0.006	0.007	0.009	0.007	0.008	0.011	0.013
B018	19.68	18.58	18.18	17.84	17.77	17.69	17.36	17.31	17.12	17.07	16.89	16.90	16.94	16.82	16.87
	0.144	0.041	0.054	0.050	0.030	0.031	0.038	0.027	0.025	0.032	0.034	0.030	0.040	0.058	0.077
B020D	...	...	18.43	18.09	17.80	17.52	17.16	17.09	16.85	16.68	16.55	16.40	16.37	16.13	16.12
	...	...	0.056	0.044	0.037	0.033	0.027	0.024	0.023	0.021	0.022	0.018	0.033	0.024	0.037
B024	...	18.55	17.87	17.66	17.16	16.84	16.48	16.43	16.30	16.20	16.02	15.83	15.94	15.80	15.77
	...	0.043	0.020	0.044	0.025	0.016	0.025	0.011	0.015	0.022	0.014	0.012	0.031	0.033	0.027
B046	...	19.23	18.66	18.36	18.21	17.85	17.39	17.45	17.29	17.15	17.02	16.81	17.03	17.20	16.70
	...	0.076	0.034	0.097	0.085	0.036	0.053	0.028	0.076	0.086	0.039	0.035	0.081	0.104	0.070
B058	17.11	16.14	15.75	15.49	15.23	15.12	14.81	14.79	14.55	14.50	14.41	14.38	14.44	14.27	14.25
	0.016	0.005	0.007	0.010	0.006	0.005	0.005	0.004	0.003	0.004	0.006	0.004	0.005	0.008	0.011
B083	19.10	18.73	17.97	17.90	17.32	17.03	16.70	16.63	16.55	16.43	16.20	15.98	16.20	16.09	15.91
	0.138	0.045	0.020	0.084	0.039	0.021	0.031	0.015	0.026	0.037	0.017	0.014	0.044	0.046	0.041
B085	18.89	17.73	17.48	17.27	17.08	16.97	16.67	16.60	16.41	16.38	16.31	16.23	16.33	16.10	16.14
	0.071	0.014	0.027	0.035	0.017	0.015	0.018	0.011	0.008	0.013	0.021	0.012	0.020	0.034	0.032
B138D	...	18.51	18.39	17.61	17.04	16.84	16.48	16.38	16.16	16.07	15.94	15.70	15.69	15.66	15.47
	...	0.050	0.021	0.035	0.023	0.012	0.015	0.009	0.007	0.012	0.010	0.010	0.013	0.019	0.018
B140D	...	19.27	18.99	18.45	18.04	17.64	17.39	17.25	16.99	16.93	16.80	16.64	16.55	16.40	16.27
	...	0.098	0.036	0.075	0.053	0.019	0.028	0.015	0.010	0.021	0.017	0.014	0.022	0.029	0.035
B141D	...	19.22	18.76	18.22	17.87	17.33	17.12	16.91	16.67	16.65	16.52	16.32	16.18	16.09	16.03
	...	0.096	0.030	0.063	0.046	0.015	0.022	0.012	0.008	0.017	0.015	0.012	0.018	0.024	0.028
B142D	18.84	19.83	19.61	19.33	18.78	18.71	18.27	18.32	18.09	18.07	18.05	17.63	18.18	17.70	17.51
	0.164	0.151	0.072	0.186	0.131	0.049	0.066	0.044	0.024	0.051	0.055	0.032	0.125	0.104	0.093
B144D	...	19.93	19.05	18.25	18.04	18.06	17.55	17.42	17.20	17.10	16.95	16.79	16.84	16.70	16.67
	...	0.176	0.041	0.060	0.050	0.025	0.032	0.017	0.012	0.024	0.019	0.017	0.034	0.038	0.048
B156D	...	18.91	18.80	18.23	18.04	17.89	17.74	17.65	17.53	17.48	17.23	17.24	17.13	17.29	17.54
	...	0.079	0.032	0.063	0.053	0.023	0.041	0.022	0.014	0.030	0.023	0.024	0.043	0.072	0.115
B157D	...	19.62	19.23	18.46	18.06	17.78	17.40	17.32	17.13	17.06	16.91	16.66	16.70	16.58	16.47
	...	0.107	0.044	0.067	0.053	0.020	0.030	0.017	0.011	0.021	0.019	0.015	0.029	0.044	0.035
B165D	...	19.14	18.79	18.17	17.97	17.78	17.60	17.48	17.28	17.07	17.10	16.87	16.79	16.90	16.64
	...	0.061	0.030	0.061	0.045	0.021	0.033	0.016	0.012	0.020	0.022	0.018	0.029	0.058	0.037
B166D	...	19.53	19.43	18.33	18.33	18.18	17.73	17.62	17.41	17.30	17.18	17.03	17.00	16.97	17.07
	...	0.055	0.147	0.065	0.037	0.039	0.038	0.022	0.012	0.020	0.035	0.020	0.029	0.052	0.089
B167D	...	19.07	18.55	18.33	18.26	17.89	17.56	17.52	17.43	17.38	17.31	17.09	17.15	17.05	17.11
	...	0.051	0.031	0.084	0.086	0.030	0.054	0.023	0.036	0.050	0.034	0.027	0.058	0.103	0.092
B172D	19.55	18.76	18.52	17.82	18.11	18.10	17.92	17.89	17.82	17.89	17.97	17.79	17.99	18.05	17.89
	0.094	0.043	0.063	0.048	0.033	0.035	0.045	0.025	0.025	0.044	0.078	0.043	0.112	0.160	0.134
B177D	20.11	19.37	18.97	18.50	18.40	18.34	18.09	17.98	17.78	17.87	17.74	17.81	18.04	17.76	17.75
	0.158	0.062	0.095	0.074	0.045	0.041	0.051	0.028	0.021	0.034	0.055	0.040	0.074	0.099	0.143
B181D	...	19.12	18.64	18.19	17.94	17.85	17.65	17.51	17.38	17.30	17.26	17.16	17.25	17.34	17.03
	...	0.074	0.028	0.055	0.038	0.023	0.036	0.017	0.017	0.026	0.025	0.030	0.054	0.057	0.062
B196	...	18.43	18.15	17.77	17.58	17.40	17.16	17.05	16.79	16.74	16.64	16.65	16.62	16.58	16.60
	...	0.071	0.021	0.027	0.025	0.022	0.039	0.021	0.011	0.034	0.020	0.015	0.037	0.048	0.035
B223D	...	...	19.31	18.64	18.10	17.94	17.39	17.29	17.03	16.94	16.70	16.60	16.48	16.44	16.20
	...	...	0.132	0.069	0.044	0.083	0.040	0.019	0.009	0.020	0.027	0.016	0.024	0.035	0.045
B240	17.13	16.39	15.93	15.69	15.50	15.35	15.11	15.00	14.85	14.78	14.68	14.59	14.61	14.56	14.48
	0.035	0.009	0.004	0.009	0.006	0.005	0.006	0.003	0.003	0.005	0.005	0.004	0.007	0.006	0.017
B244	...	19.00	18.95	18.36	18.43	18.38	17.97	17.98	17.82	17.72	17.63	17.55	17.46	17.52	17.40
	...	0.058	0.043	0.067	0.066	0.037	0.054	0.033	0.028	0.037	0.039	0.032	0.071	0.077	0.092
B245D	...	19.86	19.27	18.69	18.60	18.36	18.00	18.14	18.00	17.88	17.88	17.74	17.88	18.01	18.11
	...	0.177	0.135	0.083	0.083	0.131	0.081	0.054	0.040	0.058	0.076	0.061	0.089	0.169	0.251
B257	...	...	19.32	18.62	18.34	17.99	17.50	17.35	16.99	16.83	16.62	16.52	16.40	16.16	16.11
	...	...	0.085	0.056	0.056	0.049	0.042	0.037	0.032	0.032	0.033	0.029	0.043	0.032	0.039
B260	...	...	20.51	19.76	19.53	18.95	18.25	18.06	17.57	17.35	17.02	16.82	16.62	16.27	16.12
	...	...	0.399	0.235	0.226	0.147	0.105	0.087	0.066	0.058	0.050	0.043	0.058	0.035	0.036
B261D	19.10	18.32	18.10	17.82	17.65	17.45	17.28	17.34	17.27	17.17	17.09	16.93	17.09	16.98	17.32
	0.120	0.034	0.047	0.026	0.035	0.062	0.041	0.022	0.013	0.026	0.039	0.023	0.042	0.048	0.115

TABLE 2
CONTINUED.

Object	*a*	*b*	*c*	*d*	*e*	*f*	*g*	*h*	*i*	*j*	*k*	*m*	*n*	*o*	*p*
B266	...	...	20.00	19.47	18.86	18.67	18.05	17.93	17.63	17.49	17.30	17.14	17.02	16.91	16.83
	...	...	0.150	0.103	0.065	0.056	0.042	0.037	0.029	0.031	0.030	0.031	0.052	0.038	0.059
B270D	...	18.62	18.25	18.05	17.84	17.62	17.42	17.27	17.15	17.05	16.98	16.92	16.87	16.93	16.83
	...	0.052	0.020	0.043	0.026	0.019	0.030	0.012	0.012	0.018	0.019	0.017	0.031	0.033	0.129
B272	...	...	19.75	19.01	18.61	18.39	17.91	17.82	17.58	17.40	17.16	17.02	16.95	16.74	16.56
	...	...	0.084	0.054	0.039	0.031	0.033	0.028	0.026	0.026	0.035	0.027	0.056	0.034	0.046
B281	...	...	18.62	18.23	17.99	17.80	17.53	17.42	17.23	17.16	17.00	16.90	16.90	16.67	16.67
	...	...	0.034	0.025	0.022	0.025	0.024	0.024	0.025	0.026	0.030	0.027	0.042	0.034	0.057
B283D	18.97	18.39	18.07	17.82	17.58	17.59	17.30	17.29	17.15	17.14	17.00	16.86	16.92	16.73	16.79
	0.105	0.037	0.042	0.030	0.033	0.058	0.036	0.024	0.014	0.026	0.031	0.022	0.041	0.046	0.071
B283	...	19.45	18.66	18.42	18.03	17.89	17.55	17.47	17.27	17.18	17.04	16.93	17.07	16.78	16.80
	...	0.132	0.034	0.062	0.036	0.030	0.040	0.023	0.021	0.027	0.031	0.025	0.071	0.028	0.134
B289D	19.63	19.33	19.07	18.62	18.51	18.75	18.02	18.04	17.96	17.95	17.71	17.62	17.72	17.62	17.47
	0.180	0.068	0.100	0.053	0.076	0.169	0.077	0.039	0.025	0.053	0.071	0.042	0.083	0.078	0.142
B292D	...	19.06	19.01	18.34	18.00	17.91	17.62	17.51	17.38	17.37	17.33	17.05	17.04	17.12	16.85
	...	0.055	0.102	0.041	0.047	0.092	0.050	0.028	0.016	0.032	0.047	0.025	0.044	0.052	0.077
B292	19.01	18.18	17.81	17.43	17.29	17.22	16.96	16.90	16.76	16.70	16.70	16.54	16.58	16.43	16.46
	0.183	0.026	0.014	0.034	0.030	0.015	0.019	0.012	0.008	0.016	0.016	0.013	0.022	0.031	0.030
B293D	19.58	18.58	18.36	18.08	18.14	17.79	17.76	17.60	17.59	17.50	17.36	17.32	17.38	17.08	17.32
	0.186	0.065	0.022	0.034	0.047	0.040	0.065	0.033	0.024	0.036	0.041	0.033	0.135	0.076	0.099
B297D	...	...	19.46	18.64	18.11	17.77	17.26	17.14	16.85	16.75	16.48	16.16	16.15	16.12	15.77
	...	...	0.149	0.049	0.051	0.080	0.040	0.019	0.010	0.017	0.024	0.013	0.022	0.025	0.030
B301	19.56	18.62	18.14	17.36	17.40	17.28	16.96	16.85	16.60	16.57	16.52	16.44	16.41	16.34	16.18
	0.093	0.028	0.043	0.030	0.020	0.018	0.022	0.013	0.008	0.013	0.021	0.015	0.019	0.029	0.041
B303	19.52	18.62	18.26	17.96	18.06	18.00	18.04	17.88	17.84	18.24	18.56	18.18	18.41	18.28	18.10
	0.104	0.033	0.053	0.055	0.032	0.035	0.057	0.034	0.029	0.074	0.166	0.072	0.117	0.211	0.244
B304	18.92	17.84	17.53	17.19	17.13	16.93	16.65	16.58	16.43	16.40	16.34	16.19	16.19	16.14	16.14
	0.189	0.021	0.011	0.025	0.030	0.013	0.017	0.010	0.007	0.013	0.013	0.011	0.022	0.028	0.030
B305	19.89	19.06	18.67	17.98	18.11	18.03	17.74	17.61	17.51	17.53	17.45	17.44	17.46	17.29	16.94
	0.120	0.054	0.076	0.059	0.031	0.034	0.041	0.026	0.017	0.027	0.054	0.034	0.049	0.066	0.080
B306	19.47	18.17	17.69	16.71	16.78	16.54	16.07	15.88	15.57	15.48	15.29	15.17	15.15	14.91	14.79
	0.113	0.023	0.033	0.020	0.013	0.011	0.011	0.008	0.004	0.006	0.008	0.006	0.007	0.010	0.015
B307	19.79	18.52	18.12	17.58	17.59	17.51	17.26	17.17	16.97	16.97	16.74	16.74	16.85	16.58	16.46
	0.152	0.033	0.051	0.038	0.023	0.021	0.028	0.018	0.012	0.019	0.029	0.019	0.030	0.039	0.054
B309	19.98	18.78	18.55	17.80	17.88	17.75	17.44	17.31	17.12	17.10	17.15	17.03	17.04	17.01	17.05
	0.148	0.054	0.077	0.054	0.033	0.034	0.037	0.021	0.020	0.028	0.056	0.035	0.044	0.088	0.118
B310	18.99	18.05	17.77	17.45	17.32	17.16	16.85	16.76	16.63	16.57	16.50	16.35	16.33	16.27	16.24
	0.153	0.027	0.014	0.031	0.025	0.014	0.019	0.010	0.009	0.015	0.016	0.014	0.024	0.027	0.033
B311	17.64	16.62	16.33	15.81	15.79	15.61	15.32	15.20	14.98	14.95	14.83	14.79	14.79	14.63	14.61
	0.024	0.007	0.011	0.012	0.007	0.006	0.007	0.005	0.003	0.005	0.008	0.005	0.007	0.010	0.011
B312	18.04	16.91	16.47	16.01	15.86	15.68	15.28	15.22	15.01	14.94	14.82	14.65	14.67	14.59	14.53
	0.082	0.009	0.006	0.012	0.010	0.006	0.007	0.005	0.003	0.006	0.005	0.005	0.007	0.010	0.009
B313	18.85	17.99	17.47	16.82	16.74	16.57	16.17	16.08	15.82	15.76	15.58	15.49	15.47	15.24	15.22
	0.063	0.026	0.034	0.024	0.016	0.012	0.013	0.009	0.006	0.009	0.011	0.008	0.012	0.014	0.018
B315	17.56	16.63	16.51	16.20	16.42	16.38	16.23	16.23	16.10	16.13	16.08	16.09	16.18	16.03	15.93
	0.024	0.008	0.013	0.016	0.012	0.013	0.014	0.012	0.010	0.013	0.018	0.015	0.025	0.028	0.034
B316	...	18.28	17.75	17.25	17.24	17.21	16.95	16.82	16.67	16.65	16.55	16.57	16.60	16.48	16.42
	...	0.028	0.038	0.030	0.020	0.021	0.025	0.018	0.014	0.019	0.025	0.019	0.027	0.038	0.049
B317	18.66	17.67	17.28	17.37	16.93	16.65	16.37	16.33	16.29	16.21	16.12	15.94	16.02	15.93	15.98
	0.097	0.019	0.014	0.044	0.022	0.013	0.023	0.012	0.017	0.021	0.015	0.012	0.021	0.025	0.038
B325	18.50	17.81	17.55	17.12	17.27	17.19	16.92	16.86	16.70	16.71	16.64	16.63	16.69	16.42	16.55
	0.053	0.027	0.034	0.036	0.026	0.023	0.024	0.017	0.014	0.019	0.034	0.019	0.030	0.050	0.053
B332D	...	...	18.87	18.46	17.85	17.34	17.10	16.88	16.66	16.56	16.32	16.27	16.16	16.03	16.02
	...	...	0.036	0.064	0.027	0.015	0.023	0.010	0.008	0.014	0.016	0.013	0.021	0.014	0.067
B335	...	19.60	19.15	18.77	18.36	18.15	17.64	17.49	17.12	17.07	16.76	16.71	16.69	16.52	16.23
	...	0.101	0.132	0.116	0.053	0.050	0.047	0.033	0.024	0.031	0.040	0.024	0.029	0.051	0.046
B337	18.77	17.85	17.51	17.43	17.04	16.76	16.43	16.35	16.32	16.20	16.09	15.89	16.01	15.93	15.89
	0.100	0.027	0.015	0.046	0.021	0.014	0.021	0.010	0.012	0.028	0.013	0.011	0.018	0.031	0.031
B338	16.31	15.36	15.02	14.59	14.53	14.41	14.11	14.05	13.84	13.82	13.71	13.71	13.73	13.57	13.54
	0.011	0.005	0.005	0.006	0.004	0.003	0.004	0.003	0.002	0.003	0.004	0.003	0.003	0.005	0.008
B340D	...	...	19.39	19.59	18.15	18.64	17.79	17.58	17.23	17.31	16.93	16.83	16.74	16.66	16.76
	...	...	0.135	0.644	0.144	0.304	0.062	0.025	0.020	0.056	0.026	0.024	0.055	0.030	0.107

TABLE 2
CONTINUED.

Object	*a*	*b*	*c*	*d*	*e*	*f*	*g*	*h*	*i*	*j*	*k*	*m*	*n*	*o*	*p*
B343	18.22	17.19	16.94	16.53	16.55	16.48	16.20	16.11	15.91	15.92	15.79	15.80	15.84	15.74	15.72
	0.039	0.012	0.016	0.019	0.012	0.010	0.012	0.008	0.005	0.009	0.012	0.008	0.013	0.017	0.028
B344	18.17	17.32	16.79	16.62	16.22	15.96	15.59	15.49	15.40	15.32	15.16	14.98	15.07	14.95	14.93
	0.063	0.015	0.009	0.018	0.015	0.008	0.012	0.006	0.006	0.010	0.007	0.006	0.008	0.015	0.015
B347	18.35	17.54	17.13	17.15	16.71	16.51	16.17	16.09	16.03	15.94	15.84	15.63	15.75	15.60	15.71
	0.064	0.017	0.011	0.026	0.023	0.012	0.018	0.009	0.011	0.016	0.011	0.010	0.020	0.030	0.028
B348	19.28	18.49	17.86	17.63	17.18	16.84	16.47	16.48	16.36	16.26	16.08	15.89	15.98	15.83	15.84
	0.172	0.042	0.024	0.054	0.036	0.018	0.030	0.014	0.020	0.023	0.017	0.013	0.027	0.039	0.033
B350	18.61	17.61	17.28	16.84	16.91	16.89	16.51	16.48	16.25	16.23	16.10	16.10	16.15	15.95	16.00
	0.049	0.013	0.022	0.024	0.015	0.013	0.015	0.010	0.006	0.010	0.016	0.009	0.017	0.021	0.034
B351	19.34	18.70	18.33	18.12	17.84	17.93	17.36	17.11	17.14	17.13	17.04	16.78	16.85	16.77	16.77
	0.134	0.053	0.055	0.040	0.036	0.102	0.039	0.019	0.011	0.023	0.032	0.018	0.030	0.051	0.066
B352	18.59	17.61	17.18	17.01	16.81	16.59	16.32	16.31	16.14	16.08	16.02	15.83	15.89	15.86	15.79
	0.070	0.022	0.020	0.018	0.016	0.032	0.017	0.010	0.005	0.011	0.014	0.010	0.015	0.024	0.029
B354	19.34	18.86	18.52	18.31	18.02	18.08	17.49	17.52	17.38	17.34	17.27	17.06	17.11	16.96	16.92
	0.139	0.065	0.065	0.060	0.039	0.099	0.042	0.026	0.014	0.030	0.041	0.022	0.042	0.056	0.073
B356	19.34	18.31	17.85	17.59	17.32	17.08	16.77	16.71	16.47	16.41	16.30	16.07	16.15	16.00	16.00
	0.146	0.046	0.036	0.034	0.025	0.044	0.026	0.015	0.008	0.015	0.018	0.014	0.018	0.031	0.034
B357	18.84	18.02	17.52	17.00	16.86	16.68	16.47	16.33	16.12	16.02	15.92	15.94	15.88	15.75	15.74
	0.094	0.041	0.012	0.014	0.014	0.013	0.022	0.011	0.005	0.014	0.012	0.009	0.023	0.024	0.023
B361	18.91	17.88	17.67	17.32	17.23	17.12	16.95	16.82	16.63	16.63	16.53	16.58	16.48	16.49	16.42
	0.089	0.034	0.014	0.017	0.019	0.017	0.029	0.017	0.007	0.023	0.017	0.012	0.029	0.047	0.033
B365	18.77	17.75	17.44	17.24	16.93	16.76	16.52	16.45	16.29	16.26	16.04	15.92	15.97	15.95	15.88
	0.088	0.023	0.027	0.019	0.019	0.035	0.021	0.012	0.006	0.012	0.022	0.011	0.018	0.023	0.034
B370	18.23	17.43	17.11	16.84	16.52	16.31	16.00	15.95	15.73	15.67	15.52	15.33	15.39	15.29	15.20
	0.052	0.020	0.021	0.016	0.018	0.027	0.016	0.011	0.007	0.010	0.012	0.009	0.012	0.016	0.021
B372	18.82	17.71	17.43	17.07	16.81	16.69	16.36	16.30	16.10	16.09	15.91	15.76	15.82	15.77	15.69
	0.095	0.024	0.026	0.020	0.020	0.033	0.020	0.012	0.007	0.011	0.015	0.011	0.016	0.023	0.027
B373	18.06	17.37	16.73	16.27	15.94	15.75	15.40	15.37	15.13	15.06	14.84	14.67	14.72	14.58	14.48
	0.049	0.018	0.015	0.010	0.011	0.018	0.009	0.007	0.004	0.006	0.007	0.006	0.008	0.010	0.013
B375	...	18.92	18.51	18.34	17.92	17.73	17.38	17.32	17.13	17.02	16.87	16.78	16.85	16.66	16.48
	...	0.068	0.033	0.061	0.037	0.026	0.035	0.022	0.020	0.026	0.031	0.028	0.043	0.041	0.106
B377	19.28	18.08	17.70	17.45	17.34	17.16	17.03	16.82	16.67	16.67	16.56	16.63	16.54	16.49	16.47
	0.127	0.049	0.014	0.019	0.023	0.017	0.033	0.019	0.009	0.023	0.021	0.013	0.036	0.042	0.041
B378	...	18.49	18.38	18.18	17.80	17.65	17.36	17.42	17.23	17.17	17.05	16.91	17.09	16.97	17.05
	...	0.044	0.059	0.047	0.043	0.070	0.045	0.036	0.021	0.036	0.044	0.032	0.052	0.071	0.092
B382	...	18.51	18.01	17.87	17.59	17.42	17.19	17.10	16.96	16.89	16.77	16.66	16.71	16.70	16.80
	...	0.050	0.021	0.037	0.026	0.019	0.027	0.013	0.015	0.021	0.029	0.022	0.040	0.039	0.121
B383	18.06	17.30	16.72	16.30	16.05	15.88	15.57	15.43	15.24	15.16	14.96	14.87	14.87	14.75	14.72
	0.088	0.017	0.007	0.013	0.009	0.007	0.008	0.004	0.004	0.006	0.006	0.005	0.008	0.007	0.020
B384	18.14	17.18	16.78	16.34	16.17	16.02	15.69	15.57	15.34	15.26	15.10	15.12	15.16	14.97	14.97
	0.046	0.018	0.007	0.009	0.012	0.008	0.012	0.007	0.003	0.008	0.007	0.005	0.010	0.011	0.011
B386	17.75	16.84	16.48	16.17	15.86	15.70	15.38	15.35	15.14	15.11	14.97	14.79	14.84	14.79	14.71
	0.035	0.009	0.012	0.008	0.009	0.017	0.009	0.006	0.003	0.005	0.008	0.005	0.008	0.011	0.014
B387	19.14	17.73	17.63	17.47	17.30	17.14	16.97	16.85	16.66	16.65	16.54	16.55	16.65	16.44	16.32
	0.106	0.037	0.013	0.021	0.023	0.017	0.032	0.015	0.010	0.020	0.021	0.013	0.035	0.046	0.029
B393	...	18.25	17.83	17.54	17.26	17.09	16.80	16.69	16.53	16.49	16.33	16.25	16.21	16.14	16.03
	...	0.039	0.016	0.029	0.018	0.014	0.019	0.009	0.008	0.013	0.013	0.011	0.026	0.015	0.046
B399	...	18.38	18.05	18.01	17.58	17.45	17.23	17.14	17.03	16.92	16.82	16.79	16.91	16.78	16.90
	...	0.049	0.019	0.044	0.025	0.018	0.028	0.013	0.011	0.019	0.024	0.018	0.047	0.029	0.134
B401	18.67	17.70	17.39	17.43	17.07	16.92	16.69	16.59	16.47	16.42	16.29	16.20	16.23	16.20	16.22
	0.149	0.030	0.012	0.029	0.017	0.013	0.020	0.010	0.009	0.014	0.014	0.013	0.023	0.019	0.085
B403	18.77	17.75	17.20	17.07	16.54	16.40	16.06	15.93	15.75	15.66	15.47	15.35	15.39	15.27	15.29
	0.133	0.032	0.009	0.023	0.012	0.009	0.011	0.006	0.005	0.008	0.009	0.007	0.013	0.009	0.030
B405	17.33	16.26	15.85	15.87	15.43	15.29	15.01	14.90	14.74	14.69	14.52	14.43	14.47	14.41	14.42
	0.043	0.010	0.004	0.010	0.006	0.005	0.005	0.003	0.003	0.005	0.005	0.004	0.006	0.005	0.018
B420	...	19.36	19.18	18.45	17.91	17.67	17.36	17.20	16.98	16.90	16.79	16.56	16.50	16.48	16.20
	...	0.110	0.046	0.073	0.039	0.020	0.030	0.015	0.011	0.021	0.018	0.015	0.026	0.035	0.032
B448	19.60	18.24	18.15	17.92	17.95	17.89	17.59	17.58	17.44	17.40	17.45	17.38	17.40	17.44	17.18
	0.136	0.037	0.060	0.067	0.052	0.058	0.055	0.050	0.048	0.054	0.069	0.059	0.071	0.121	0.088
B457	19.20	18.25	17.91	17.90	17.48	17.21	16.91	16.84	16.76	16.66	16.55	16.35	16.42	16.44	16.43
	0.139	0.041	0.020	0.072	0.034	0.021	0.035	0.015	0.023	0.039	0.019	0.017	0.045	0.061	0.051

TABLE 2
CONTINUED.

Object	*a*	*b*	*c*	*d*	*e*	*f*	*g*	*h*	*i*	*j*	*k*	*m*	*n*	*o*	*p*
B461	19.41	18.91	18.38	18.15	17.67	17.49	17.09	16.99	16.85	16.78	16.62	16.41	16.54	16.39	16.43
	0.157	0.056	0.027	0.067	0.047	0.020	0.036	0.016	0.018	0.034	0.017	0.014	0.026	0.050	0.054
B462	...	19.03	18.77	18.67	18.42	18.19	17.80	17.74	17.66	17.52	17.45	17.30	17.44	17.29	17.37
	...	0.063	0.040	0.112	0.092	0.036	0.065	0.030	0.036	0.061	0.032	0.027	0.058	0.090	0.130
B467	...	18.57	18.25	18.00	17.83	17.51	17.35	17.25	17.11	17.02	17.08	16.82	16.86	16.75	16.84
	...	0.052	0.052	0.044	0.035	0.060	0.039	0.021	0.012	0.024	0.038	0.019	0.032	0.046	0.063
B472	17.60	16.43	16.00	15.68	15.40	15.25	14.95	14.89	14.75	14.66	14.58	14.46	14.40	14.35	14.35
	0.025	0.024	0.009	0.007	0.006	0.006	0.006	0.006	0.006	0.006	0.007	0.006	0.009	0.008	0.012
B475	19.38	18.08	17.74	17.66	17.50	17.36	17.28	17.37	17.21	17.17	17.00	16.97	16.95	16.71	16.57
	0.156	0.047	0.050	0.054	0.062	0.074	0.066	0.069	0.053	0.061	0.076	0.061	0.067	0.068	0.071
B476	...	...	19.26	18.87	18.72	18.50	18.14	18.12	17.95	17.87	17.70	17.49	17.68	17.46	17.68
	...	...	0.064	0.093	0.076	0.050	0.068	0.037	0.037	0.053	0.070	0.054	0.096	0.083	0.254
B483	...	18.86	18.62	18.49	18.32	18.17	18.33	18.11	18.13	18.20	18.11	17.86	18.03	18.07	17.58
	...	0.059	0.071	0.054	0.062	0.103	0.096	0.044	0.039	0.069	0.095	0.055	0.099	0.130	0.146
B486	...	18.68	18.19	18.03	17.83	17.65	17.48	17.40	17.23	17.15	17.11	17.05	17.03	16.89	16.86
	...	0.055	0.019	0.042	0.027	0.019	0.031	0.014	0.014	0.023	0.021	0.020	0.058	0.036	0.123
B489	...	19.32	18.88	18.01	17.65	17.33	17.12	16.91	16.70	16.57	16.40	16.32	16.26	16.15	15.98
	...	0.112	0.033	0.035	0.036	0.030	0.041	0.020	0.010	0.021	0.022	0.013	0.052	0.034	0.035
B495	...	...	19.59	18.82	18.16	17.95	17.38	17.19	16.94	16.85	16.58	16.34	16.26	16.22	15.93
	...	...	0.160	0.075	0.046	0.077	0.039	0.020	0.009	0.019	0.020	0.013	0.021	0.028	0.034
G260	19.07	18.05	17.75	17.57	17.22	17.11	16.79	16.74	16.62	16.58	16.45	16.25	16.29	16.28	16.26
	0.112	0.027	0.034	0.025	0.023	0.041	0.025	0.013	0.007	0.015	0.023	0.013	0.023	0.031	0.047

TABLE 3
GALEX, OPTICAL BROAD-BAND, AND 2MASS NIR PHOTOMETRY OF 104 M31 GCS AND GC CANDIDATES.

Object	c†	FUV	NUV	U	B	V	R	I	J	H	K_s
B001	1	...	...	18.82	18.33	17.06	16.47	15.41	14.69	13.73	13.84
		...	...	0.08	0.05	0.05	0.05	0.05	0.04	0.04	0.05
B003	1	23.06	21.55	18.40	18.35	17.57	17.07	16.41	15.95	15.15	15.51
		0.20	0.04	0.04	0.02	0.01	0.03	0.02	0.08	0.10	0.12
B005	1	...	21.08	16.12	16.04	15.44	14.99	14.66	13.40	12.69	12.51
		...	0.12	0.02	0.01	0.01	0.01	0.01	0.03	0.03	0.03
B018	1	...	22.09	18.47	18.25	17.53	17.00	16.38	15.47	14.77	14.59
		...	0.15	0.08	0.05	0.05	0.05	0.05	0.08	0.07	0.10
B020D	1	...	...	18.99	18.43	17.44	...	16.04	14.91	14.62	13.98
		...	...	0.08	0.05	0.05	...	0.05	0.04	0.07	0.05
B024	1	...	22.51	18.40	17.75	16.80	16.27	15.65	14.80	14.25	13.98
		...	0.07	0.08	0.02	0.01	0.01	0.01	0.04	0.07	0.05
B046	1	22.80	21.71	18.70	18.65	17.81	17.37	16.87	15.91	14.83	14.93
		0.16	0.05	0.09	0.03	0.01	0.04	0.03	0.08	0.07	0.10
B058	1	20.23	19.09	16.05	15.81	15.01	14.48	13.91	13.13	12.50	12.36
		0.04	0.01	0.01	0.01	0.01	0.01	0.01	0.03	0.03	0.03
B083	1	22.60	21.45	17.91	17.85	17.09	16.55	15.93	15.32	14.61	14.59
		0.14	0.03	0.04	0.02	0.01	0.02	0.01	0.08	0.07	0.10
B085	1	22.24	20.60	17.92	17.55	16.84	16.38	15.63	15.03	14.72	14.29
		0.11	0.03	0.08	0.05	0.05	0.05	0.05	0.08	0.07	0.10
B138D	2	23.11	22.38	18.70	17.92	16.87	16.14	...	14.24	13.48	13.18
		0.18	0.06	0.08	0.05	0.05	0.05	...	0.04	0.04	0.05
B140D	2	22.31	21.73	18.74	18.87	17.67	17.04	...	15.17	14.45	13.99
		0.08	0.05	0.08	0.05	0.05	0.05	...	0.08	0.07	0.05
B141D	2	...	...	18.89	18.73	17.43	16.69	...	14.75	14.04	13.55
		...	...	0.08	0.05	0.05	0.05	...	0.04	0.07	0.05
B142D	2	21.21	21.21	19.06	19.80	18.63	17.93	...	16.99	...	14.98
		0.10	0.07	0.08	0.05	0.05	0.05	...	0.10	...	0.10
B144D	2	...	...	19.37	18.85	17.72	17.06	...	15.70	15.02	14.96
		...	...	0.08	0.05	0.05	0.05	...	0.08	0.10	0.10
B156D	2	20.97	20.29	18.57	18.88	18.16	17.49	...	16.15	...	15.18
		0.04	0.02	0.08	0.05	0.05	0.05	...	0.10	...	0.12
B157D	2	...	...	19.37	19.06	17.83	17.24	...	15.19	14.62	14.03
		...	...	0.08	0.05	0.05	0.05	...	0.08	0.07	0.10
B165D	2	21.06	20.82	18.92	18.68	17.62	17.34	...	15.63	14.72	14.19
		0.06	0.04	0.08	0.05	0.05	0.05	...	0.08	0.07	0.10
B166D	2	...	...	19.11	18.90	17.93	17.34	...	15.47	14.83	14.41
		...	...	0.08	0.05	0.05	0.05	...	0.08	0.07	0.10
B167D	1	22.09	21.34	18.41	18.54	17.79	17.31	...	16.36	15.65	15.28
		0.07	0.03	0.08	0.05	0.05	0.05	...	0.10	0.10	0.12
B172D	2	...	21.71	18.44	18.64	17.97	17.61	...	...	...	...
		...	0.08	0.08	0.05	0.05	0.05	...	...	...	...
B177D	2	...	...	19.11	18.89	18.09	17.63	...	...	...	...
		...	...	0.08	0.05	0.05	0.05	...	...	...	...
B181D	2	...	...	18.73	18.71	17.72	17.14	...	15.24	16.41	...
		...	...	0.08	0.05	0.05	0.05	...	0.08	0.10	...
B196	1	...	21.60	18.35	18.05	17.40	16.75	16.10	15.54	14.57	14.82
		...	0.10	0.08	0.05	0.05	0.05	0.05	0.08	0.07	0.10
B223D	2	...	22.86	19.30	18.74	17.75	...	...	15.25	14.19	13.81
		...	0.13	0.08	0.05	0.05	...	...	0.08	0.07	0.05
B240	1	19.90	18.94	16.03	15.93	15.23	14.73	14.20	13.47	12.90	12.76
		0.04	0.01	0.01	0.01	0.01	0.01	0.01	0.03	0.03	0.03
B244	2	...	22.23	19.13	19.05	18.27	17.66	17.22	15.46	15.36	...
		...	0.07	0.08	0.04	0.01	0.05	0.04	0.08	0.10	...
B245D	2	...	...	18.91	19.08	18.22	17.56	...	16.20	16.65	...
		...	...	0.08	0.05	0.05	0.05	...	0.10	0.10	...
B257	2	...	...	19.75	19.43	20.96	...	16.31	14.79	13.98	13.69
		...	...	0.08	0.05	0.05	...	0.05	0.04	0.04	0.05
B260	2	...	...	...	...	18.50	17.52	16.42	14.69	13.90	13.74
		...	...	...	...	0.01	0.01	0.07	0.04	0.04	0.05

†New classification flag (RBC v.3.5): 1 = GC, 2 = candidate GC.

TABLE 3
CONTINUED.

Object	c†	FUV	NUV	U	B	V	R	I	J	H	K_s
B261D	2	...	21.31	18.02	18.06	17.60	16.97	...	15.35	15.38	...
		...	0.04	0.08	0.05	0.05	0.05	...	0.08	0.10	...
B266	1	...	...	18.76	19.29	18.32	17.40	16.50	15.64	15.06	14.45
		...	...	0.08	0.05	0.05	0.05	0.05	0.08	0.10	0.10
B270D	2	...	21.81	18.24	17.90	17.50	16.94	...	15.43	15.09	...
		...	0.07	0.08	0.05	0.05	0.05	...	0.08	0.10	...
B272	1	...	...	19.94	19.52	18.20	17.50	16.61	14.70	14.40	...
		...	...	0.08	0.06	0.01	0.05	0.05	0.04	0.07	...
B281	1	...	...	19.01	18.51	17.67	17.11	16.51	15.87	14.88	14.26
		...	...	0.06	0.03	0.01	0.03	0.03	0.08	0.07	0.10
B283D	2	...	21.02	18.11	18.12	17.51	16.97	...	15.16	14.87	...
		...	0.03	0.08	0.05	0.05	0.05	...	0.08	0.07	...
B283	1	...	...	19.63	18.70	17.64	17.20	16.53	15.73	14.90	15.05
		...	...	0.08	0.04	0.01	0.03	0.02	0.08	0.07	0.12
B289D	1	...	...	18.94	18.94	18.09	17.74	...	15.49	...	...
		...	...	0.08	0.05	0.05	0.05	...	0.08	...	...
B292D	1	...	...	18.95	18.89	17.81	...	...	15.39	15.25	...
		...	...	0.08	0.05	0.05	...	...	0.08	0.10	...
B292	1	21.80	21.02	17.87	17.89	17.00	16.62	16.06	15.41	15.03	14.71
		0.09	0.03	0.08	0.05	0.05	0.05	0.05	0.08	0.10	0.10
B293D	2	...	21.32	18.33	18.45	17.91	17.29	...	16.52	15.99	15.41
		...	0.05	0.08	0.05	0.05	0.05	...	0.10	0.10	0.12
B297D	2	...	...	20.06	19.05	17.63	...	...	14.66	13.90	13.70
		...	...	0.08	0.05	0.05	...	...	0.04	0.04	0.05
B301	1	...	...	18.48	18.13	17.12	16.53	15.71	15.08	14.31	14.06
		...	...	0.08	0.05	0.05	0.05	0.05	0.08	0.07	0.10
B303	1	...	21.15	18.92	18.46	18.22	17.50	17.03	...	...	...
		...	0.05	0.08	0.05	0.05	0.05	0.05	...	...	...
B304	1	22.03	20.69	17.78	17.54	16.83	16.32	15.74	15.12	14.46	14.27
		0.08	0.03	0.08	0.05	0.05	0.05	0.05	0.08	0.07	0.10
B305	1	...	22.69	18.68	18.82	17.93	17.21	17.00	15.80	15.48	15.34
		...	0.18	0.08	0.05	0.05	0.05	0.05	0.08	0.10	0.12
B306	1	...	22.31	18.19	17.55	16.30	15.59	14.63	13.55	12.74	12.58
		...	0.15	0.08	0.05	0.01	0.05	0.01	0.03	0.03	0.03
B307	1	...	21.84	19.20	18.19	17.32	17.15	16.10	15.22	14.56	14.18
		...	0.08	0.08	0.05	0.01	0.05	0.01	0.08	0.07	0.10
B309	1	...	22.00	18.63	18.47	17.50	17.00	15.80	16.01	...	15.92
		...	0.10	0.08	0.05	0.05	0.05	0.05	0.10	...	0.12
B310	1	22.03	20.87	18.03	17.80	17.04	16.54	15.98	15.24	14.65	14.63
		0.08	0.03	0.08	0.05	0.05	0.05	0.05	0.08	0.07	0.10
B311	1	21.18	19.72	16.55	16.41	15.44	14.94	14.22	13.50	12.86	12.70
		0.06	0.02	0.08	0.05	0.05	0.05	0.05	0.03	0.03	0.03
B312	1	21.06	20.08	16.68	16.34	15.52	14.96	14.16	13.56	12.85	12.78
		0.10	0.04	0.08	0.05	0.05	0.05	0.05	0.03	0.03	0.03
B313	1	...	20.77	18.11	17.41	16.37	15.79	14.96	14.06	13.30	13.11
		...	0.12	0.08	0.05	0.05	0.05	0.05	0.04	0.04	0.05
B315	1	18.70	18.36	16.57	16.55	16.47	16.03	15.58	14.82	14.67	13.98
		0.02	0.01	0.08	0.05	0.05	0.05	0.05	0.04	0.07	0.05
B316	1	...	...	18.10	17.77	17.06	16.39	16.14	14.71	14.43	...
		...	...	0.08	0.02	0.01	0.02	0.02	0.04	0.07	...
B317	1	21.67	20.27	17.58	17.30	16.57	16.13	15.71	14.98	14.53	14.50
		0.05	0.01	0.08	0.05	0.05	0.05	0.05	0.04	0.07	0.10
B325	1	19.93	...	...	17.54	16.94	16.42	15.91	15.22	14.57	14.38
		0.06	...	...	0.02	0.01	0.02	0.02	0.08	0.07	0.10
B332D	2	...	...	19.02	18.70	17.21	16.60	...	14.81	13.86	13.55
		...	...	0.08	0.05	0.05	0.05	...	0.04	0.04	0.05
B335	1	...	...	19.99	19.04	17.89	16.91	16.14	14.94	14.24	13.94
		...	...	0.08	0.06	0.01	0.04	0.03	0.04	0.07	0.05
B337	1	21.89	20.70	17.69	17.52	16.73	16.24	15.63	15.06	14.47	14.06
		0.06	0.02	0.08	0.05	0.05	0.05	0.05	0.08	0.07	0.10

†New classification flag (RBC v.3.5): 1 = GC, 2 = candidate GC.

TABLE 3
CONTINUED.

Object	c†	FUV	NUV	U	B	V	R	I	J	H	K_s
B338	1	19.05	18.28	15.21	15.06	14.30	13.67	13.28	12.45	11.79	11.67
		0.02	0.01	0.01	0.01	0.01	0.05	0.01	0.02	0.02	0.02
B340D	2	...	...	20.22	19.93	17.92	17.22	...	15.53	14.55	14.45
		...	...	0.08	0.05	0.05	0.05	...	0.08	0.07	0.10
B343	1	20.80	19.90	17.23	17.08	16.31	15.91	15.27	14.63	13.94	13.90
		0.06	0.02	0.08	0.05	0.05	0.05	0.05	0.04	0.04	0.05
B344	1	...	20.75	17.01	16.77	15.95	15.33	14.87	14.02	13.40	13.35
		...	0.02	0.08	0.05	0.01	0.05	0.01	0.04	0.04	0.05
B347	1	22.10	20.26	17.38	17.23	16.50	15.97	15.49	14.75	14.04	14.11
		0.08	0.02	0.08	0.05	0.01	0.05	0.01	0.04	0.07	0.10
B348	1	...	22.06	18.33	17.98	16.79	16.33	15.64	14.78	14.34	13.93
		...	0.07	0.08	0.05	0.01	0.05	0.01	0.04	0.07	0.05
B350	1	21.77	20.47	17.47	17.36	16.74	16.20	15.64	14.84	14.46	14.19
		0.08	0.03	0.08	0.05	0.01	0.05	0.01	0.04	0.07	0.10
B351	1	...	21.67	18.61	18.40	17.55	17.07	16.43	15.98	15.22	14.88
		...	0.04	0.08	0.05	0.05	0.05	0.05	0.08	0.10	0.10
B352	1	21.11	20.08	17.42	17.25	16.54	15.96	15.57	14.93	14.28	14.11
		0.05	0.02	0.08	0.05	0.05	0.05	0.05	0.04	0.07	0.10
B354	1	...	21.69	18.63	17.94	17.81	17.19	16.74	16.01	15.21	15.25
		...	0.05	0.08	0.05	0.01	0.05	0.02	0.10	0.10	0.12
B356	1	22.33	21.43	18.42	18.12	17.34	16.43	15.71	14.93	14.29	14.24
		0.17	0.05	0.08	0.05	0.05	0.05	0.05	0.04	0.07	0.10
B357	1	...	21.81	17.98	17.49	16.61	15.97	15.39	14.48	13.80	13.68
		...	0.07	0.08	0.05	0.05	0.05	0.05	0.04	0.04	0.05
B361	1	21.40	20.54	17.92	17.78	17.05	16.57	16.01	15.32	14.71	14.56
		0.07	0.03	0.08	0.05	0.05	0.05	0.05	0.08	0.07	0.10
B365	1	21.64	20.58	17.72	17.51	16.72	15.90	15.57	14.97	14.24	14.10
		0.05	0.02	0.08	0.05	0.05	0.05	0.05	0.04	0.07	0.10
B370	1	21.48	20.53	17.28	17.15	16.30	15.63	15.14	14.17	13.44	13.34
		0.05	0.02	0.03	0.01	0.01	0.01	0.01	0.04	0.04	0.05
B372	1	...	20.97	17.71	17.48	16.60	15.84	15.50	14.68	13.95	13.80
		...	0.04	0.08	0.05	0.05	0.05	0.05	0.04	0.04	0.05
B373	1	...	21.23	17.07	16.58	15.64	15.13	14.39	13.36	12.57	12.46
		...	0.07	0.03	0.01	0.01	0.01	0.01	0.03	0.03	0.03
B375	1	...	22.44	19.87	18.51	17.61	17.07	16.59	15.49	14.68	14.32
		...	0.19	0.08	0.03	0.01	0.03	0.04	0.08	0.07	0.10
B377	1	...	20.70	17.83	17.77	17.14	16.64	16.20	15.43	15.09	14.44
		...	0.05	0.08	0.05	0.05	0.05	0.05	0.08	0.10	0.10
B378	1	...	21.49	18.85	18.52	17.83	16.94	16.50	15.99	15.40	15.19
		...	0.05	0.08	0.05	0.05	0.05	0.05	0.08	0.10	0.12
B382	1	21.91	20.97	18.28	18.15	17.36	16.74	16.08	15.69	15.09	15.52
		0.10	0.04	0.08	0.05	0.05	0.05	0.05	0.08	0.10	0.12
B383	1	...	21.21	17.23	16.17	15.33	14.87	14.43	13.58	12.85	12.66
		...	0.06	0.08	0.05	0.05	0.05	0.05	0.03	0.03	0.03
B384	1	...	21.32	17.37	16.74	15.75	15.26	14.56	13.76	13.01	12.91
		...	0.07	0.08	0.05	0.05	0.05	0.05	0.03	0.04	0.03
B386	1	21.64	20.00	16.68	16.45	15.55	14.75	14.39	13.70	12.95	12.83
		0.08	0.02	0.08	0.05	0.05	0.05	0.05	0.03	0.03	0.03
B387	1	...	20.69	17.84	17.66	16.98	16.48	16.05	15.32	14.94	14.43
		...	0.05	0.08	0.05	0.05	0.05	0.05	0.08	0.07	0.10
B393	1	...	21.75	17.97	17.72	16.93	16.40	16.00	15.18	14.23	14.21
		...	0.09	0.08	0.05	0.05	0.05	0.05	0.08	0.07	0.10
B399	1	...	21.00	18.25	18.05	17.28	16.85	16.23	15.80	15.50	15.35
		...	0.08	0.08	0.05	0.05	0.05	0.05	0.08	0.10	0.12
B401	1	...	20.43	17.83	17.51	16.83	16.50	15.68	15.09	14.60	14.56
		...	0.05	0.08	0.05	0.05	0.05	0.05	0.08	0.07	0.10
B403	1	...	21.59	17.62	17.19	16.22	15.68	15.00	14.15	13.48	13.24
		...	0.11	0.08	0.05	0.05	0.05	0.05	0.04	0.04	0.05
B405	1	19.72	18.89	16.22	15.93	15.19	14.66	...	13.41	12.77	12.66
		0.06	0.02	0.08	0.05	0.05	0.05	...	0.03	0.03	0.03

†New classification flag (RBC v.3.5): 1 = GC, 2 = candidate GC.

TABLE 3
CONTINUED.

Object	c†	FUV	NUV	U	B	V	R	I	J	H	K_s
B420	2	...	...	19.68	18.96	17.85	17.12	16.13	15.16	14.68	14.15
		...	...	0.08	0.05	0.05	0.05	0.05	0.08	0.07	0.10
B448	1	21.90	21.14	18.11	18.10	17.49	17.06	16.77	...	...	...
		0.12	0.05	0.09	0.04	0.01	0.04	0.03	...	...	...
B457	1	...	21.21	18.05	17.73	16.91	16.38	16.87	14.68	14.78	...
		...	0.03	0.08	0.05	0.05	0.05	0.05	0.04	0.07	...
B461	1	...	22.82	18.73	18.77	17.52	16.89	16.04	15.55	14.67	14.61
		...	0.14	0.08	0.05	0.05	0.05	0.05	0.08	0.07	0.10
B462	1	...	21.96	18.82	18.83	18.06	17.38	17.01	15.45	...	...
		...	0.06	0.08	0.05	0.01	0.05	0.02	0.08	...	...
B467	1	22.49	21.33	18.36	18.31	17.43	16.85	16.15	15.96	15.73	15.18
		0.10	0.03	0.08	0.05	0.05	0.05	0.05	0.08	0.10	0.12
B472	1	19.93	19.03	16.16	15.97	15.19	14.67	14.12	13.34	12.69	12.60
		0.04	0.02	0.01	0.01	0.01	0.01	0.01	0.03	0.03	0.03
B475	1	...	21.07	17.97	17.87	17.56	17.03	16.91	16.04	15.01	14.63
		...	0.06	0.10	0.03	0.01	0.04	0.04	0.10	0.10	0.10
B476	2	...	...	19.52	19.12	18.12	17.69	17.00	15.34	14.68	...
		...	...	0.09	0.05	0.01	0.06	0.05	0.08	0.07	...
B483	1	...	21.73	18.81	18.73	18.46	17.75	17.82	...	...	...
		...	0.05	0.08	0.05	0.05	0.05	0.05	...	...	...
B486	1	...	21.36	18.80	17.87	17.52	17.03	16.49	15.90	15.54	15.46
		...	0.09	0.08	0.05	0.05	0.05	0.05	0.08	0.10	0.12
B489	2	...	...	19.32	18.47	17.35	16.66	15.64	14.76	13.99	13.80
		...	...	0.08	0.05	0.05	0.05	0.05	0.04	0.04	0.05
B495	2	...	...	19.60	19.02	17.61	17.04	15.82	14.83	14.02	13.74
		...	...	0.08	0.05	0.05	0.05	0.05	0.04	0.07	0.05
G260	1	22.69	21.11	17.64	17.81	17.01	16.53	...	15.25	14.80	14.59
		0.13	0.04	0.08	0.05	0.05	0.05	...	0.08	0.07	0.10

†New classification flag (RBC v.3.5): 1 = GC, 2 = candidate GC.

TABLE 4
REDDENING VALUES (MAGNITUDES) AND METALLICITIES (DEX) FOR 104 M31 GCS AND GC CANDIDATES.

Object	$E(B-V)$	ref.[a]	[Fe/H]	ref.[b]
B001	0.25± 0.02	1	−0.58± 0.18	1
B003	0.19± 0.02	1	−2.08± 0.07	4
B005	0.28± 0.02	1	−1.18± 0.17	1
B018	0.20± 0.01	1	−1.63± 0.77	1
B020D	0.22± 0.06	1	−0.76± 0.08	4
B024	0.03± 0.02	1	−0.48± 0.30	3
B046	0.19± 0.03	1	−1.84± 0.61	3
B058	0.13± 0.01	1	−1.45± 0.24	3
B083	0.12± 0.02	1	−1.18± 0.44	1
B085	0.14± 0.02	1	−1.83± 0.40	3
B138D	0.23± 0.04	1	−0.36± 0.04	4
B140D	0.45± 0.11	1	−1.57± 0.12	4
B141D	0.43± 0.09	1	−1.07± 0.08	4
B142D	0.58± 0.03	1	−2.59± 0.24	4
B144D	0.33± 0.02	1	−1.62± 0.09	4
B156D	0.45± 0.09	1	−2.58± 0.14	4
B157D	0.15± 0.01	1	−0.09± 0.08	4
B165D	0.21± 0.07	1	−1.05± 0.13	4
B166D	0.26± 0.04	1	−1.02± 0.08	4
B167D	0.23± 0.03	1	−2.34± 0.08	4
B172D	0.11± 0.05	1	−2.51± 0.12	4
B177D	0.08± 0.02	1	−1.32± 0.01	4
B181D	0.36± 0.09	1	−2.21± 0.20	4
B196	0.26± 0.04	1	−1.94± 0.08	4
B223D	0.20± 0.05	1	−0.23± 0.08	4
B240	0.13± 0.00	1	−1.76± 0.18	3
B244	0.27± 0.03	1	−1.50± 0.21	4
B245D	0.52± 0.03	1	−2.88± 0.09	4
B257	1.17± 0.03	1	−2.05± 0.82	4
B260	0.67± 0.02	1	−0.36± 0.10	4
B261D	0.27± 0.06	1	−2.45± 0.19	4
B266	0.98± 0.09	1	−2.80± 0.15	4
B270D	0.25± 0.02	1	−2.28± 0.19	4
B272	0.57± 0.04	1	−1.25± 0.16	1
B281	0.12± 0.02	1	−0.87± 0.52	1
B283D	0.16± 0.04	1	−1.55± 0.17	4
B283	0.08± 0.06	2	−0.06± 0.20	1
B289D	0.23± 0.05	1	−1.71± 0.63	1
B292D	0.23± 0.14	2	−0.47± 0.54	1
B292	0.23± 0.14	2	−1.42± 0.16	2
B293D	0.27± 0.06	1	−2.57± 0.11	4
B297D	0.30± 0.07	1	0.10± 0.08	4
B301	0.17± 0.02	1	−0.76± 0.25	1
B303	0.14± 0.06	1	−2.09± 0.41	1
B304	0.07± 0.01	1	−1.32± 0.22	2
B305	0.38± 0.29	2	−0.90± 0.61	1
B306	0.42± 0.02	1	−0.85± 0.71	1
B307	0.08± 0.02	1	−0.41± 0.36	1
B309	0.17± 0.04	1	−2.03± 0.26	4
B310	0.09± 0.01	1	−1.43± 0.28	2
B311	0.29± 0.02	1	−1.96± 0.07	1
B312	0.16± 0.01	1	−1.41± 0.08	1

[a]The reddening values are taken from Fan et al. (2008) (ref=1) and Barmby et al. (2000) (ref=2).
[b]The metallicities are taken from Perrett et al. (2002) (ref=1), Barmby et al. (2000) (ref=2), Huchra et al. (1991) (ref=3), and Fan et al. (2008) (ref=4).

Table 4
Contintuted.

Object	$E(B-V)$	ref.[a]	[Fe/H]	ref.[b]
B313	0.21± 0.02	1	−1.09± 0.10	1
B315	0.07± 0.02	1	−2.35± 0.54	1
B316	0.21± 0.03	1	−1.47± 0.23	1
B317	0.11± 0.02	1	−2.12± 0.36	3
B325	0.14± 0.02	1	−1.77± 0.08	4
B332D	0.33± 0.13	1	−0.65± 0.09	4
B335	0.65± 0.02	1	−1.05± 0.26	1
B337	0.06± 0.02	1	−1.09± 0.32	2
B338	0.14± 0.02	1	−1.46± 0.12	1
B340D	0.23± 0.06	1	0.19± 0.29	4
B343	0.06± 0.01	1	−1.49± 0.17	3
B344	0.11± 0.02	1	−1.13± 0.21	3
B347	0.14± 0.02	1	−1.71± 0.03	4
B348	0.25± 0.04	1	−1.38± 0.07	4
B350	0.10± 0.02	1	−1.47± 0.17	2
B351	0.15± 0.02	1	−1.60± 0.05	4
B352	0.14± 0.02	1	−1.88± 0.83	3
B354	0.05± 0.02	1	−1.46± 0.38	2
B356	0.31± 0.01	1	−1.46± 0.28	1
B357	0.12± 0.02	1	−0.80± 0.42	3
B361	0.11± 0.01	1	−1.61± 0.02	4
B365	0.19± 0.02	1	−1.78± 0.19	1
B370	0.34± 0.01	1	−1.80± 0.02	1
B372	0.20± 0.02	1	−1.42± 0.17	1
B373	0.10± 0.01	1	−0.50± 0.22	3
B375	0.29± 0.03	1	−1.23± 0.22	3
B377	0.16± 0.02	1	−2.19± 0.65	3
B378	0.14± 0.02	1	−1.64± 0.26	1
B382	0.10± 0.02	1	−1.52± 0.27	1
B383	0.00± 0.02	2	−0.48± 0.20	2
B384	0.04± 0.02	1	−0.66± 0.22	3
B386	0.21± 0.01	1	−1.62± 0.14	1
B387	0.12± 0.02	1	−1.96± 0.29	3
B393	0.14± 0.02	1	−1.41± 0.05	4
B399	0.03± 0.02	1	−1.69± 0.09	4
B401	0.06± 0.06	2	−1.75± 0.29	2
B403	0.07± 0.02	1	−0.45± 0.78	3
B405	0.14± 0.02	1	−1.80± 0.31	3
B420	0.30± 0.03	1	−0.63± 0.07	4
B448	0.05± 0.01	1	−2.16± 0.19	1
B457	0.14± 0.02	1	−1.60± 0.21	4
B461	0.58± 0.07	1	−2.56± 0.07	4
B462	0.39± 0.04	1	−2.28± 0.34	4
B467	0.27± 0.02	1	−2.49± 0.47	1
B472	0.13± 0.00	1	−1.45± 0.02	1
B475	0.16± 0.03	1	−2.00± 0.14	1
B476	0.08± 0.05	1	−0.03± 0.13	4
B483	0.08± 0.06	1	−2.96± 0.35	1
B486	0.17± 0.02	1	−2.28± 0.98	3
B489	0.17± 0.04	1	−0.04± 0.10	4
B495	0.34± 0.08	1	−0.35± 0.05	4
G260	0.30± 0.05	1	−2.45± 0.06	4

[a]The reddening values are taken from Fan et al. (2008) (ref=1) and Barmby et al. (2000) (ref=2).
[b]The metallicities are taken from Perrett et al. (2002) (ref=1), Barmby et al. (2000) (ref=2), Huchra et al. (1991) (ref=3), and Fan et al. (2008) (ref=4).

TABLE 5
AGES ESTIMATES FOR 104 GCS AND GC CANDIDATES IN M31.

Object	Age (Gyr)	$\chi^2_{\rm min}$ (per degree of freedom)	Object	Age (Gyr)	$\chi^2_{\rm min}$ (per degree of freedom)
B001	10.51 ± 0.80	2.79	B313	7.28 ± 0.70	5.48
B003	2.01 ± 0.20	2.10	B315	0.50 ± 0.10	7.88
B005	1.60 ± 0.10	18.92	B316	1.06 ± 0.10	7.81
B018	1.79 ± 0.20	2.74	B317	2.06 ± 0.15	2.59
B020D	8.41 ± 1.70	1.29	B325	0.40 ± 0.10	5.28
B024	15.25 ± 0.75	2.96	B332D	11.30 ± 0.85	4.33
B046	1.30 ± 0.10	5.71	B335	1.17 ± 0.15	3.55
B058	2.02 ± 0.10	2.41	B337	2.03 ± 0.10	5.66
B083	2.89 ± 0.20	10.25	B338	1.70 ± 0.10	2.43
B085	2.18 ± 0.20	2.39	B340D	13.57 ± 1.45	9.68
B138D	2.95 ± 0.35	8.09	B343	1.82 ± 0.10	2.82
B140D	0.39 ± 0.10	12.18	B344	12.68 ± 2.35	2.60
B141D	4.76 ± 1.00	3.78	B347	2.53 ± 0.15	3.23
B142D	0.03 ± 0.01	18.34	B348	6.58 ± 0.70	3.28
B144D	14.36 ± 0.95	3.36	B350	1.99 ± 0.10	2.25
B156D	0.10 ± 0.01	22.86	B351	3.20 ± 0.40	2.26
B157D	8.00 ± 1.05	3.81	B352	1.51 ± 0.10	1.16
B165D	0.50 ± 0.10	20.62	B354	5.24 ± 0.65	3.85
B166D	3.73 ± 0.90	3.26	B356	1.21 ± 0.10	3.16
B167D	0.90 ± 0.10	3.22	B357	4.98 ± 0.60	2.94
B172D	1.00 ± 0.10	10.73	B361	1.57 ± 0.10	1.40
B177D	1.70 ± 0.30	3.32	B365	1.73 ± 0.10	1.89
B181D	0.63 ± 0.15	7.72	B370	1.10 ± 0.10	3.17
B196	1.62 ± 0.10	2.39	B372	2.34 ± 0.35	1.54
B223D	4.03 ± 0.35	6.13	B373	7.79 ± 0.40	1.02
B240	1.79 ± 0.10	1.05	B375	2.19 ± 0.30	7.62
B244	0.90 ± 0.10	6.33	B377	1.09 ± 0.10	1.81
B245D	0.10 ± 0.01	7.58	B378	2.12 ± 0.30	3.70
B257	0.10 ± 0.01	6.16	B382	1.83 ± 0.15	3.33
B260	14.30 ± 0.50	1.26	B383	13.99 ± 1.05	4.73
B261D	0.57 ± 0.10	6.91	B384	10.27 ± 0.95	4.29
B266	0.03 ± 0.01	10.36	B386	2.54 ± 0.15	1.93
B270D	1.00 ± 0.10	4.01	B387	1.62 ± 0.10	2.66
B272	3.73 ± 0.90	5.10	B393	6.76 ± 1.10	1.17
B281	5.97 ± 1.30	1.97	B399	5.59 ± 0.50	2.03
B283D	1.09 ± 0.10	3.84	B401	3.49 ± 0.40	2.55
B283	2.83 ± 0.35	4.99	B403	6.39 ± 0.40	2.56
B289D	0.81 ± 0.25	2.20	B405	1.30 ± 0.10	2.97
B292D	1.15 ± 0.15	4.49	B420	10.90 ± 0.40	4.86
B292	1.00 ± 0.10	2.53	B448	1.70 ± 0.10	6.19
B293D	0.50 ± 0.10	3.90	B457	3.16 ± 0.35	12.00
B297D	15.18 ± 0.85	3.37	B461	0.56 ± 0.10	9.51
B301	2.20 ± 0.30	4.06	B462	0.50 ± 0.10	4.38
B303	0.50 ± 0.10	17.86	B467	1.00 ± 0.10	5.95
B304	2.20 ± 0.10	1.36	B472	1.30 ± 0.10	5.15
B305	0.40 ± 0.10	9.52	B475	0.97 ± 0.10	6.69
B306	3.39 ± 0.50	4.61	B476	3.14 ± 0.35	7.65
B307	1.61 ± 0.10	7.46	B483	1.00 ± 0.10	6.49
B309	4.66 ± 0.55	10.39	B486	1.61 ± 0.10	3.31
B310	2.07 ± 0.15	1.35	B489	9.07 ± 1.30	3.56
B311	1.62 ± 0.10	4.21	B495	14.54 ± 0.55	2.81
B312	2.56 ± 0.25	7.27	G260	1.00 ± 0.10	5.84

TABLE 6
AGE COMPARISON

Object	Age (Gyr) (Caldwell et al. 2009)	Age (Gyr) (this paper)
B018	1.00	1.79 ± 0.20
B303	0.40	0.50 ± 0.10
B307	1.00	1.61 ± 0.10
B315	0.16	0.50 ± 0.10
B316	1.00	1.06 ± 0.10
B325	0.63	0.40 ± 0.10
B448	0.25	1.70 ± 0.10
B475	0.32	0.97 ± 0.10
B483	0.50	1.00 ± 0.10